DEPARTMENT OF PHYSICS
COLLEGE OF SCIENCES
OLD DOMINION UNIVERSITY
NORFOLK, VIRGINIA 23529

THE SIMULATED SPACE PROTON ENVIRONMENT FOR RADIATION EFFECTS ON SPACE TELESCOPE IMAGING SPECTROGRAPH (STIS)

By

Jacob Becher, Principal Investigator

and

Walter Fowler, Research Associate

Progress Report
For the period April 16, 1991 to April 15, 1992

Prepared for
National Aeronautics and Space Administration
Goddard Space Flight Center
Greeenbelt, Maryland 20771

Under
Research Grant NAG-5-1527
Dr. Randy A. Kimble, Technical Monitor
Laboratory for Astronomy and Solar Physics

Submitted by the
Old Dominion University Research Foundation
P.O. Box 6369
Norfolk, Virginia 23508-0369

August 1992

EFFECTS OF SIMULATED SPACE PROTON ENVIRONMENT ON TRANSMISSION OF OPTICAL MATERIALS FOR THE SPACE TELESCOPE IMAGING SPECTROGRAPH (STIS)

Introduction

STIS is a second generation instrument planned for the Hubble Space Telescope (HST) which is currently in orbit (594 km perigee, 601 km apogee, and 28. 47 degree inclination). Candidate glasses and other transmitting materials are being considered for order sorters, in-flight calibration filters, detector windows and calibration lamps. It is well known that some materials undergo changes in spectral transmission characteristics with radiation dosage during a mission lifetime. It is therefore essential to study and evaluate potential materials for the STIS mission, keeping in mind the environment and the duration of mission. To this end a preliminary list of candidates was prepared by R. A. Woodruff of Ball Aerospace. These include glasses for order sorters, flight calibration filters, and general purpose window materials. Table 1 lists these materials. To proceed with the evaluation tests, one inch square samples of candidates were obtained for the purpose of subjecting them to a simulated STIS environment.

The Hubble Radiation Environment

The radiation environment was analyzed by E. G. Stassinopoulos (Reference 1) for solar minimum and solar maximum using two methods: method 1 proposed by himself and method 2 by the Committee on Radiation Models and Evaluation. Method 1 predicts a higher radiation dosage assuming a spherical shielding of 2 gms/cm^2 This amount of shielding stops all, or substantially all electrons which are projected for the environment. At lesser shielding thickness , electrons can be above the Cerenkov threshold with resultant undesirable flashes around pulse counting detectors. For the preliminary evaluations of the radiation environment for the interior of the STIS instrument, a 2 gms/cm^2 spherical shielding model was used to modify the radiation data for a 593 km altitude, 28 degree inclination orbit as described by Stassinopoulos. Figure 1 shows depth dependent dose curves for solar minimum. From the Stassinopoulos tables, dosage for protons is 0.392 Krad(Al) /Yr. and .0217 Krad (Al) /Yr. for solar minimum and solar maximum respectively. Internal proton differential flux at 2 gm/ cm^2 spectra is plotted in Figure 2. Dosage from galactic cosmic rays and solar flares is insignificant. To simulate the mission radiation environment Harvard Cyclotron Laboratory (HCL) has been used.

Simulation of Orbital Exposure at Harvard Cyclotron Laboratory

A. M. Koehler of HCL has designed a attenuator wheel to simulate a proton

spectrum representing the inside of a spacecraft passing through the South Atlantic Anomaly (SAA). This spectrum produced after the wheel is calculated for 1.1 gms/cm^2 shielding with a peak at about 35 MeV, as seen in Figure 3 (Reference 2). This is a fairly good approximation to the STIS orbit environment with a shielding of 2 gms/cm^2 where the peak is around 45 MeV as seen in Figure 2.

The 125 Mev monoenergetic cyclotron beam is converted to an energy spread beam by means of a range modulator (Reference 3). This is a large circular disk which turns about an axis parallel to the extracted cyclotron beam. The circular disk is made from an acrylic plastic with an outer portion of varying thickness intercepting the beam much like a circular light chopper and acting like a varying attenuator degrading the beam. The angular sectors were designed to develop the desired energy spectrum during each complete turn of the modulator.

For our work a beam diameter of 7 inches was used. Typical beam uniformity is shown in Figure 4. The samples for irradiation were mounted in small paper envelopes, a row of three with a row of two above and below. The area of exposure avoided beam peaks at the profile edges. All samples of this group were given 3 Krad (Si), 1.5×10^{10} p/cm^2, approximately the same as 3 Krad (Al), in an exposure time of about ten minutes. Since we expected a 0.4 Krad/Yr. as the approximate dose rate in orbit, this represents 7.5 years at solar minimum, a good value to detect problems for a five year mission.

Measurement of Spectral Transmission

Spectral transmission was measured between 210 nm and 3200 nm using a Perkin Elmer Lambda 9 monochromater. Below 210 nm a one meter McPherson vacuum monochromater was used. Transmission curves for all samples were obtained before irradiation. To simplify presentation of data here Lambda 9 before and after irradiation curves were made on a single plot using the irradiated sample and an unirradiated sample to simulate the initial curve. In all cases but one a match with the pre irradiation was possible. The exception was Optovac magnesium fluoride where only a single sample was available. The transmission curves are presented in appendix 1; the solid lines represent the transmission of the unirradiated sample whereas the broken lines represent the irradiated samples. Comparison measurements were also made before and after proton irradiation to confirm instrumentation reproducibility.

Comments on Individual Samples

The transmission data of tested samples are presented in the order of onset of transmissivity as a function of wavelength.

Optovac and Solon Industries MgF_2

Magnesium fluoride is of particular interest since it transmits down to 110 nm and its characteristics seem to vary with the manufacturer. For example the Optovac sample exhibited higher transmission than the sample from Solon Industries with an initial transmission of 61% at 121.6 nm compared to a 47% transmission for the Solon Industries sample. The Optovac showed a greater degradation estimated by a factor of

a factor of 2. Both samples after irradiation showed the beginning of F-center absorption at 260 nm, a band in magnesium fluoride that was studied at Old Dominion University in 1982 (Reference 4). Figure 5 from that study shows a drop of nearly 20% in an Optovac sample, but with 28 times the dosage used here.

Suprasil 1

The Suprasil 1 measured with the Lambda 9 monochromater showed no change in the regions 200 nm-700 nm and 800 nm-3200 nm whereas there was a 1% degradation in the 700 nm-800 nm region. Measurements with the McPherson vacuum monochromator in the region 160 nm-210 nm indicate less than 2 % degradation.

UV transmissive samples

Onset in the range 200 nm-310 nm, (Samples: Hoya UV-22, UV-28, Schott UBK-7, Hoya UV-30, Schott WG 305, Schott WG-320) have been tested.Most show small degradation of about 1% to 3% over most of the spectral range. Maximum degradation was 8% for Hoya UV-30 at about 310 nm. It is worth noting that glass samples Hoya UV-28, and Schott UBK-7 have identical transmissions before and after irradiation, having a maximum degradation of 2% at about 320 nm; and glasses Hoya UV-30, Schott WG 305 have similar absorption edges; Hoya UV-30 is vulnerable to radiation, while Schott WG-305 (which does not have as sharp a cut-off at the same wavelength) is more resistant .

UV Schott BK 7G-25, and BK 7G-18

These two glasses showed identical transmission characteristics and no deterioration due to the radiation.

Filters with transmission onset between 550 nm and 600 nm

These glasses are resistant to radiation in the visible and the near IR and for the rest of the spectral range with the exception of samples from Hoya O-54,O-56,O-58 in the region 2200 nm-3200 nm. The Schott OG-550, OG-570, and OG-590 have the same short wavelength cut-off as the Hoya samples without the degradation in the IR. It is worth noting that glass samples Schott OG-590, Hoya O-54, and Kopp 2-63 have identical transmissions onsets in the visible whereas the IR cutoff varies with Hoya having the best transmission and the highest response to irradiation.

Blocking visual band filters

Transmission proved to be unstable in these UV bandpass filter materials. Their IR curves show no degradation whereas the bandpass portion showed a 5% to 8% degradation . The glass samples tested were Schott BG-24A, BG-3, BG-1.

Conclusions and Future Possibilities

The glasses for in-flight calibration filters showed significant drop in UV transmission, but can probably still be used on STIS. The exact effect of this degradation over the mission life should be considered when interpreting spacecraft data. The cut-off absorption edge in order sorter glasses should be evaluated carefully if used as interference filter blockers.

Proton flux in the Hubble orbit is not nearly as severe as many orbits now proposed. Those which pass through the proton belt rather than the SAA receive a much stronger dose. It would be useful for these missions to have transmission curves for these samples at much higher dosage in order to evaluate the degradation

characteristics. For a start we can use the data here for 7.5 year at 0.4 Krad/year, and extrapolate for a higher range of dosages. We need to examine annealing characteristics in order to determine the effect on the missions. Finally these samples should be used in fluorescence and phosphorescence studies.

References

1. Stassinopoulos, E. G., Smith, R. L., Crabtree, C. M.," HST Radiation Exposure Evaluation," NASA X-600-89-5, (August 1989).

2. Koehler, A. M. , 1989, Private Communication.

3. Koehler, A. M., Sneider, R. J., Sisterson, J. M., "Range Modulators for Protons and Heavy Ions," Nuclear Instruments and Methods, 131, 437-440, (1975).

4, Becher, J., Kernell, R. L., Reft, C. S., " Proton Induced F-Centers in Liz and MgF2, " J Phy Chem Solids, 44, 759-763, (1983).

Acknowledgement

The authors wish to acknowledge help of the Goddard Space Flight Center Optics Branch (Code 717) on whose monochromaters most of these measurements were made and in particular assistance and advice of Howard Herzig and Charles Fleetwood.

This work was supported by NASA Grant NAG 5-1527

Evaluation of Stanford Developed Decode Chips and Integrated Charge Amplifier

The initial effort of this project was to assist in the evaluation of a 299 pin decode chip for the MAMA detector. Consideration had to be given to what should be measured and what is possible at a remote site such as the Harvard Cyclotron Laboratory (HCL). The importance of making these measurements was to determine whether the existing decoder chip could be used or there exists a need for designing a new radiation hardened decoder chip for the flight instrument. With this in mind, a special rig was constructed and the appropriate electronics brought to HCL for the test. Drs. David Kasle and Jeff Morgan of Stanford collected data to determine any timing variations in the decoder coincidence circuitry while a proton beam simulating the South Atlantic Anomaly (SAA) was impinging on the decoder chip, using dosage and dose rates comparable to the Hubble orbit, and eventually increasing the rate . No effects were noted at a fluence rate of eight times peak SAA. Then we proceeded to test if the stored codes in the memory of the chip had been affected. To this end three chips were given three dosage levels: 3.95 Krad (Si), 7.9 Krad (Si) , and 23.7 Krad (Si) for examination at Stanford since a sufficient number of test lines could not be provided at HCL to test all possible types of inputs. The memory withstood the test; the only effect found in post radiation testing was a 5% drop in speed.

The second part of the MAMA detector tested at HCL was a charge amplifier discriminator with a rig provided by Ball. The amplifier showed occasional proton

induced noise pulses at three times peak SAA. Using the provided data for peak SAA we were able to estimate the potential counts for normal operation and found them to be within acceptable limits. Then a test was performed to examine whether the noise level or the operational gain was affected by the radiation. To provide an extreme test the amplifier was subjected to a dosage of 12.5 Krad (Si) which corresponds to about 30 year, since a year's dosage for the Hubble orbit with 2 gm/cm^2 is 0.4 Krad (Si). The results were very satisfying since no change in either noise or gain was detected. A detailed description of the radiated parts and test results has been submitted by Kasle and Morgan in a letter form.

Coordination of Activities

STIS radiation program requires information transfer and coordination of activities between Dr. Bruce Woodgate, Goddard Code 683, and the Janesick group at JPL, the STIS group at BASD, the MAMA program at Stanford, and at two locations in the Washington area: (1) the NRL group (Dale, Marshall and Peterson) and (2) GSFC: Leidecker Code 313, Stassinopoulos Code 633, Hertzig Code 717, Adolfsen Code 310, and LaBel Code 735. Each of the above contributes to the total effort in a different way. In order to develop critical areas of effort Old Dominion organized a meeting which was held at GSFC on June 5. Jacob Becher of Old Dominion reviewed past programs for IUE, HRS and the approach to STIS problems. Dale and Marshall of NRL presented their analysis of displacement damage in CCDs. Randy Kimble of GSFC discussed the Janesick RTI parameter as it will apply to our evaluation of CCD displacement damage. Fowler of Old Dominion and Leidecker of GSFC discussed

Walt Viehman's phosphorescence work. This meeting allowed various parties to review related problems and programs that have common interests.

A second meeting was held in Boulder on July 23. Walter Fowler met with Richard Greenwall, Alan Delamere, Bob Woodruff and other Ball personnel. Shielding options were discussed and results of Ball shielding studies using the slab shielding model were presented by Brent Cummings. Differences were considered with shielding results for the HRS calculated by Armstrong assuming a spherical model.

Additional Radiation Tests

The FOS detector on the Hubble Space Telescope has shown symptoms which may be due to a drop of window transmission in a 20 nm band centered around 195 nm. A prototype spare window, suprasil, was irradiated at Harvard for one year's dosage. Another sample was irradiated to 7.5 years' dosage. Preliminary examination of these windows has shown no degradation, suggesting that the drop in transmission is not caused by protons.

In addition to windows and blocking glasses, three one micron thick windows of polyamide were similarly irradiated with dosage of 0.4, 2, and 5.5 Krad (Si). The main purpose for these tests was to determine leakage survival;no leakage was observed. These three detector windows are for an X-ray proportional counter on the AXAF Bragg Crystal Spectrometer. Under Dr. Seppo Nanonen of MIT these windows had previously undergone shake tests.

TABLE 1
Samples for Proton Irradiation

For order sorters:

Schott	Hoya	Kopp
WG 305	UV-22	3-66
WG 320	UV-28	2-73
OG 550	UV-30	2-63
OG 570	O-54	2-62
OG 590	O-56	
	O-58	

For in flight calibration filters:

Schott		
BG-1	BG-3 *	BG 24A

For general use:
Heraeus: Suprasil 1
Optovac, Solon Industries: Magnesium Fluoride
Schott: BK-7G 18, BK-7G 25, and UBK-7

* A similar glass substituted for BG-2 on the original list

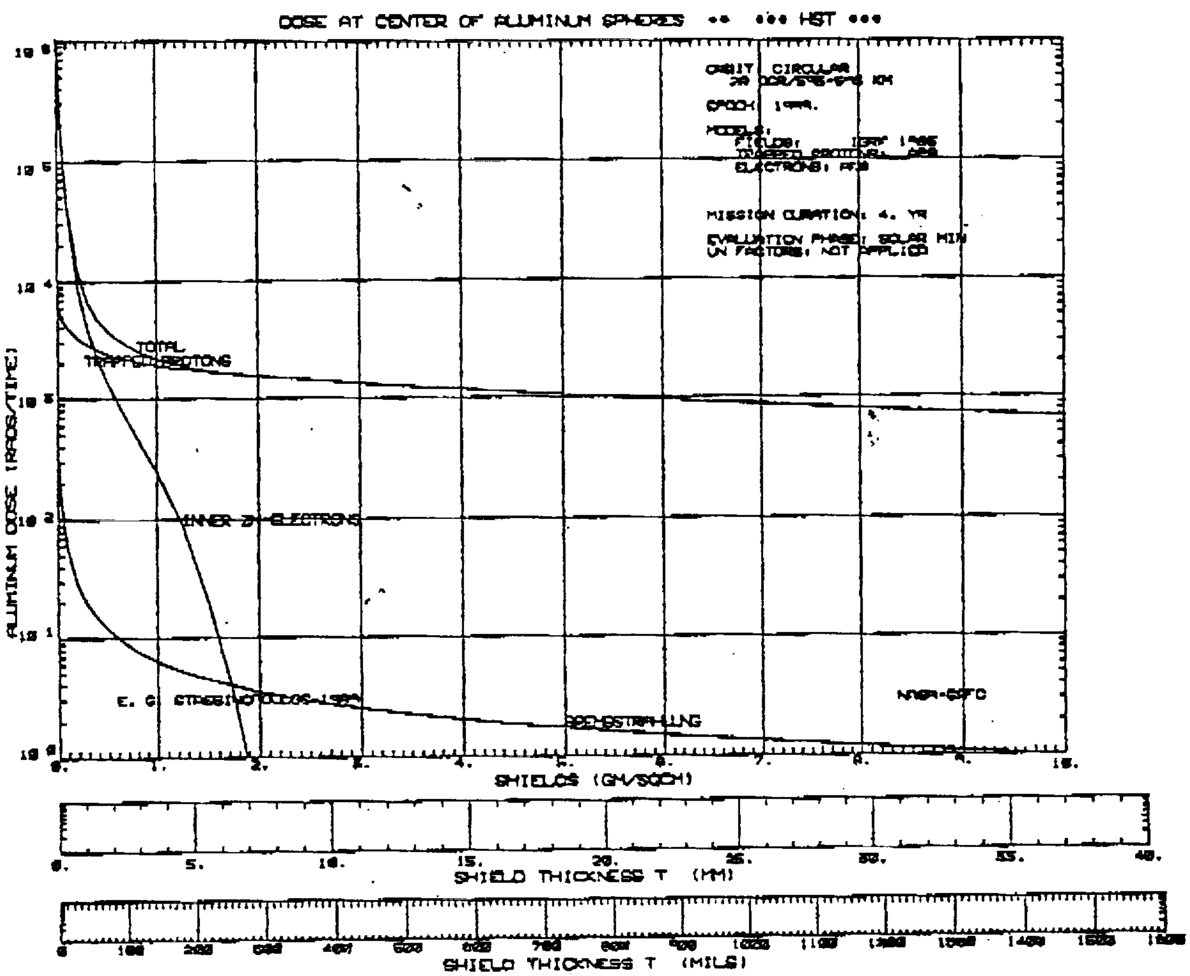
DOSE AT CENTER OF ALUMINUM SPHERES
HST
ALUMINUM DOSE (RADS/TIME)
TOTAL
TRAPPED PROTONS
SHIELDS (GM/SQCM)
SHIELD THICKNESS T (MM)
SHIELD THICKNESS T (MILS)

Figure 1

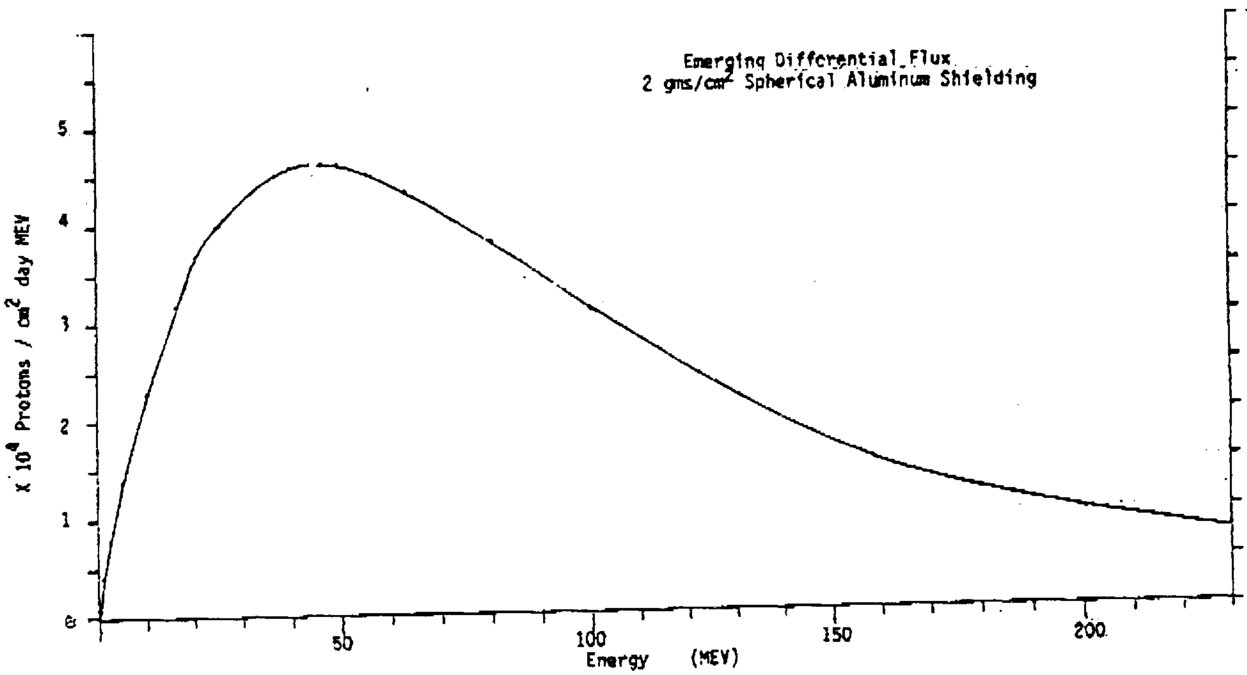
Emerging Differential Flux
2 gms/cm² Spherical Aluminum Shielding
X 10⁴ Protons / cm² day MEV
5
4
3
2
1
0
50
100
150
200
Energy (MEV)

Figure 2

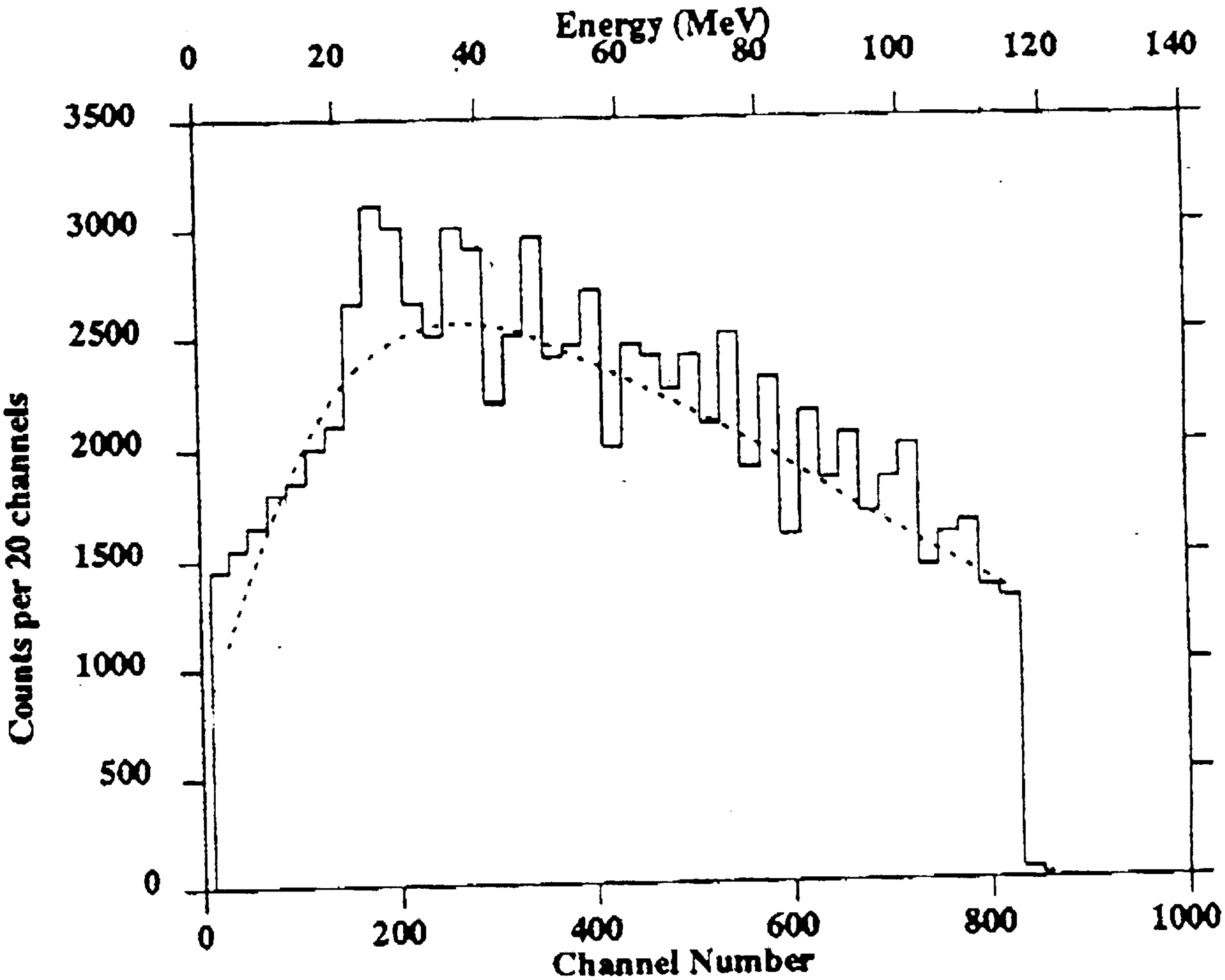
Energy (MeV)
0
20
40
60
80
100
120
140
3500
3000
2500
2000
1500
1000
500
0
Counts per 20 channels
0
200
400
600
800
1000
Channel Number

Figure 3

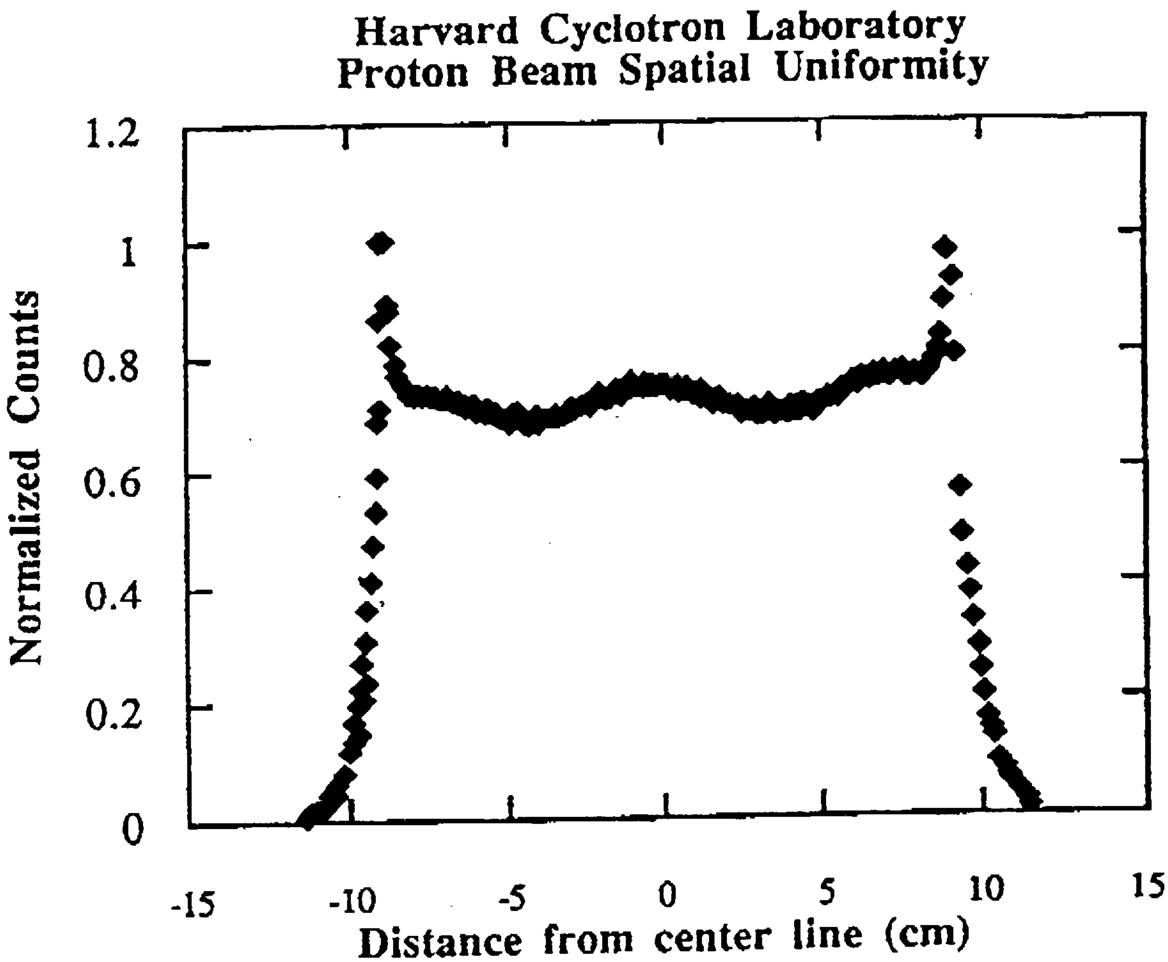
Harvard Cyclotron Laboratory
Proton Beam Spatial Uniformity
Normalized Counts
1.2
1
0.8
0.6
0.4
0.2
0
-15
-10
-5
0
5
10
15
Distance from center line (cm)

Figure 4

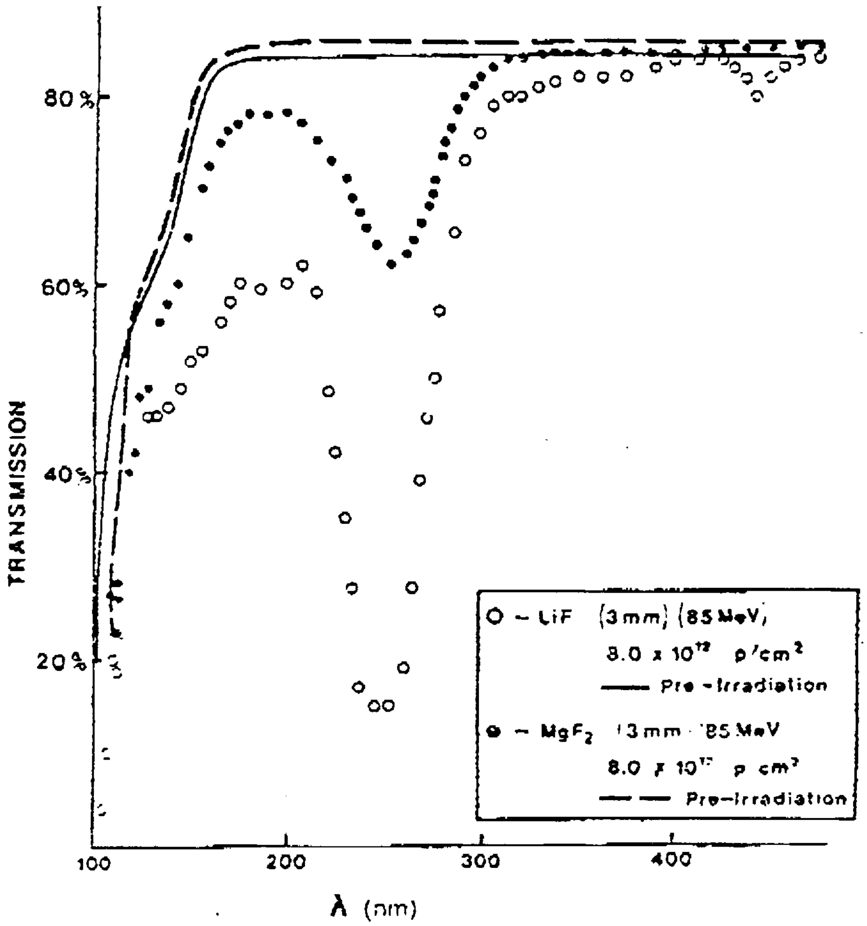

TRANSMISSION
80%
60%
40%
20%
100
200
300
400
λ (nm)
O – LiF (3mm) (85 MeV)
8.0 x 10^12 p/cm^2
Pre-Irradiation
● – MgF₂ (3mm) (85 MeV)
8.0 x 10 p cm²
Pre-Irradiation

Figure 5

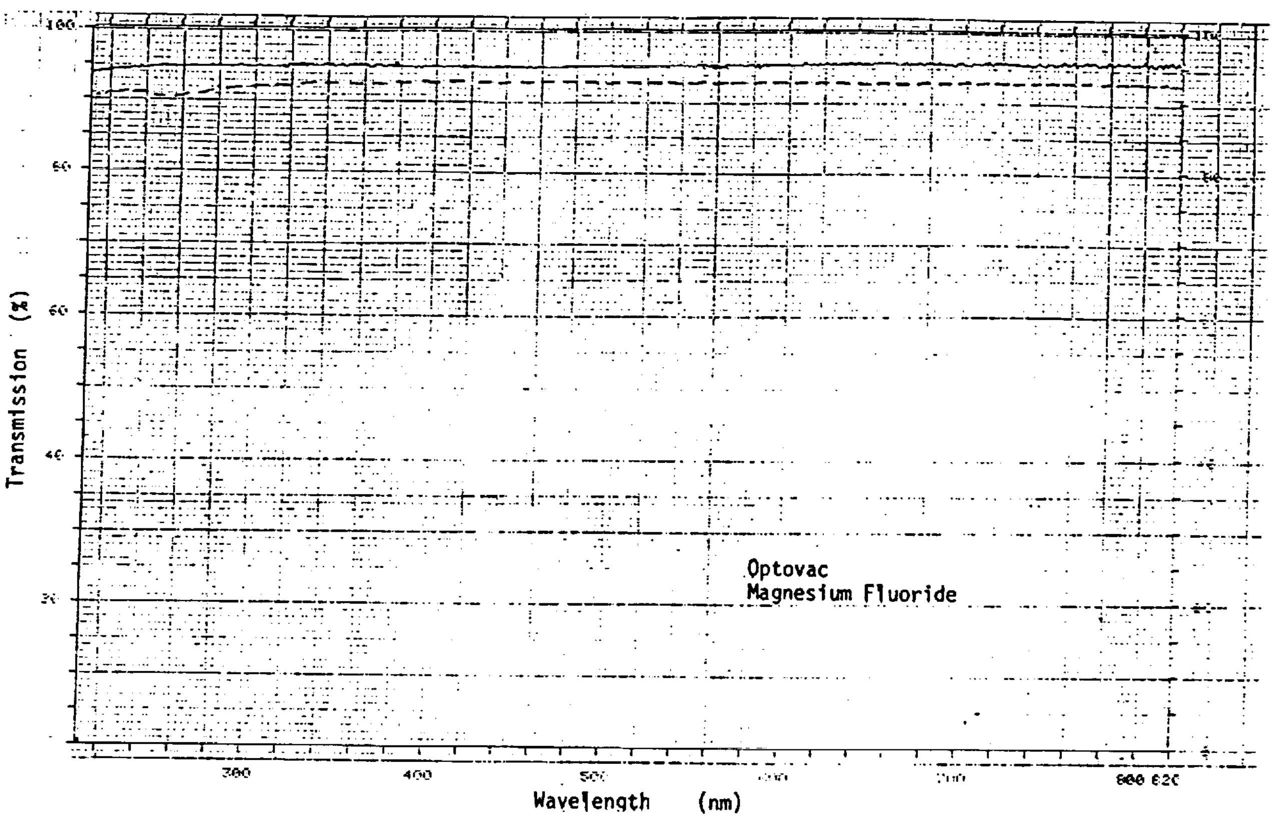
Transmission (%)
Wavelength (nm)
Optovac
Magnesium Fluoride

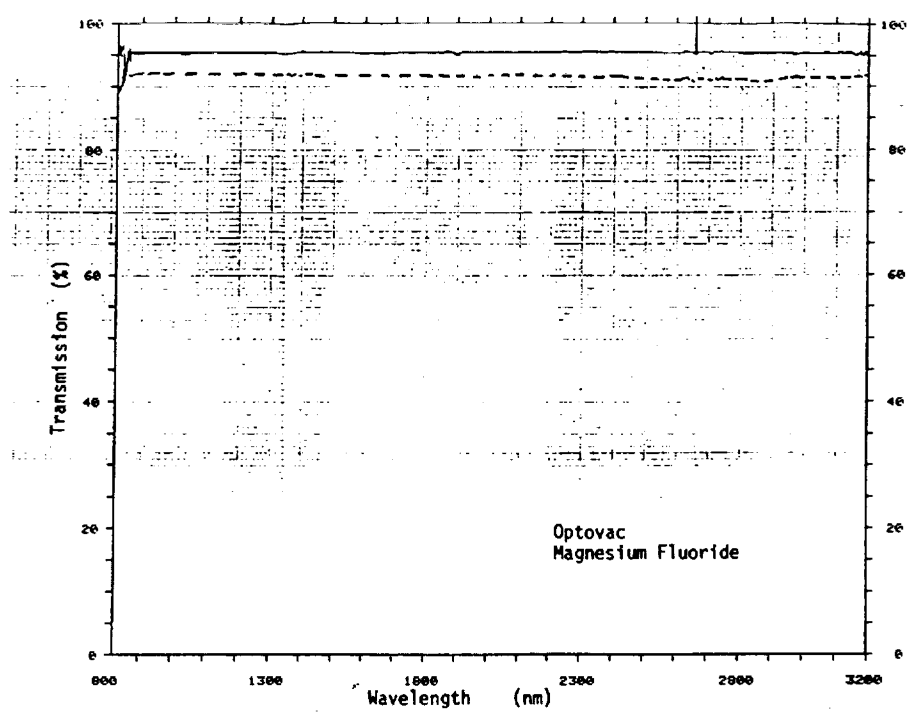
Transmission (%)
Wavelength (nm)
Optovac
Magnesium Fluoride
800
1300
1800
2300
2800
3200

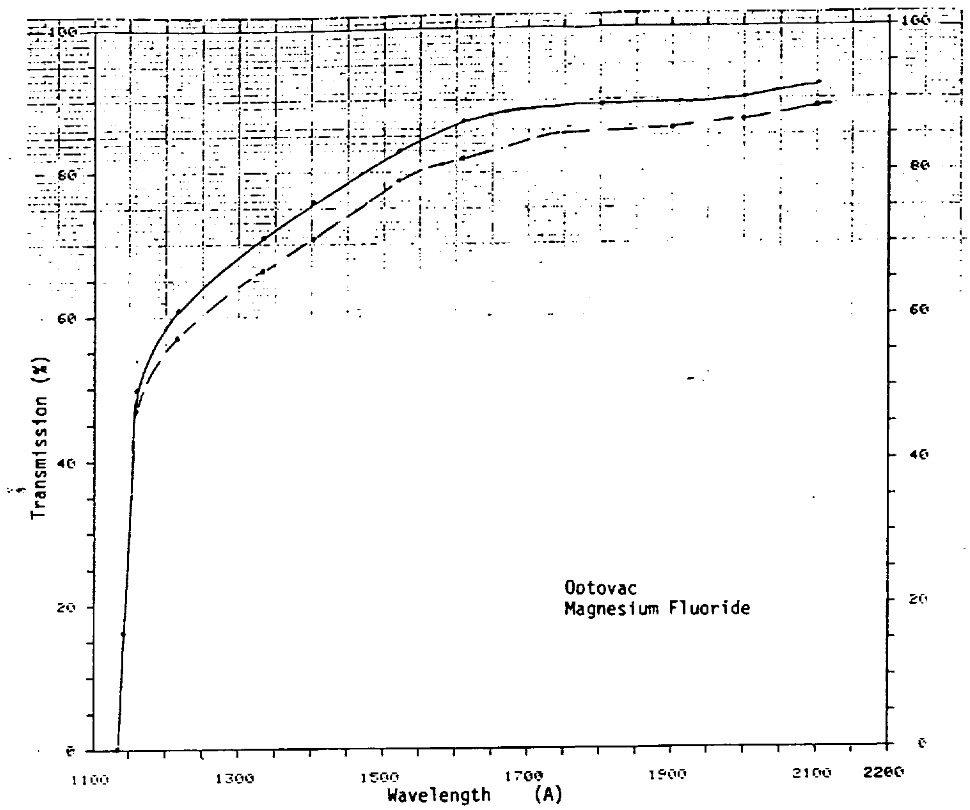

Transmission (%)
Wavelength (A)
Ootovac
Magnesium Fluoride

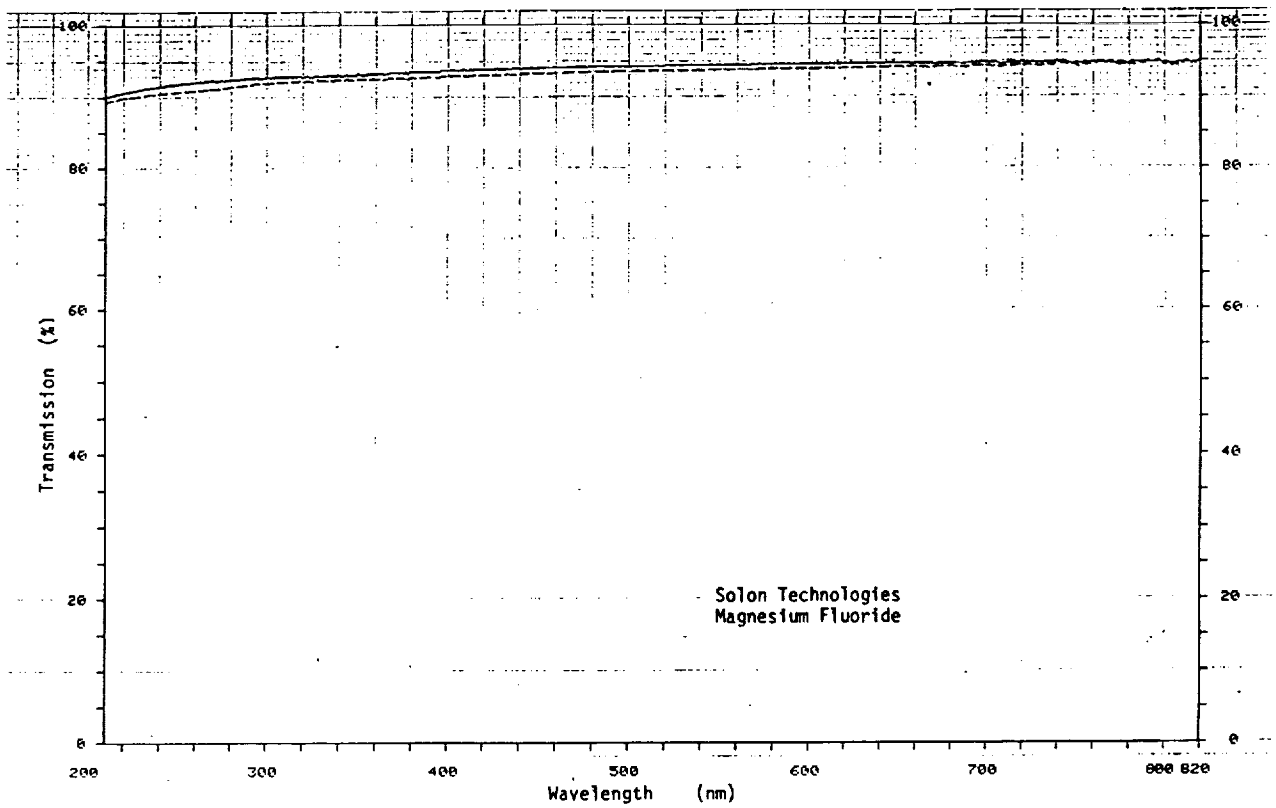
Transmission (%)
Wavelength (nm)
Solon Technologies
Magnesium Fluoride

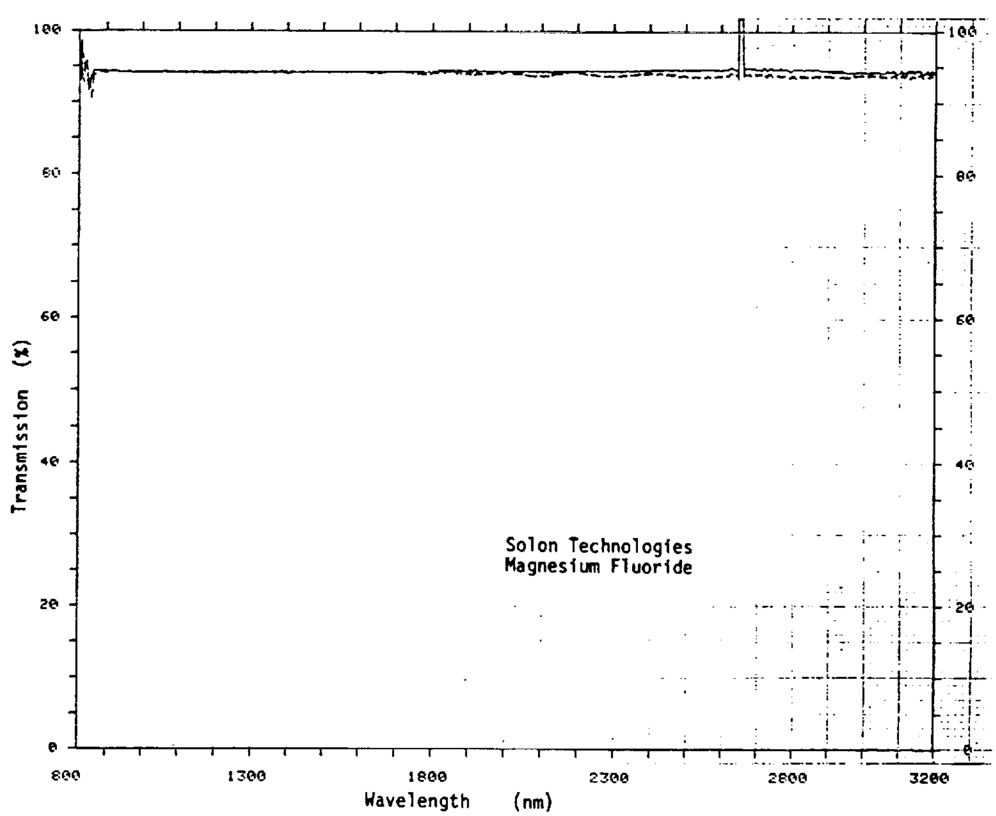
Transmission (%)
Wavelength (nm)
Solon Technologies
Magnesium Fluoride

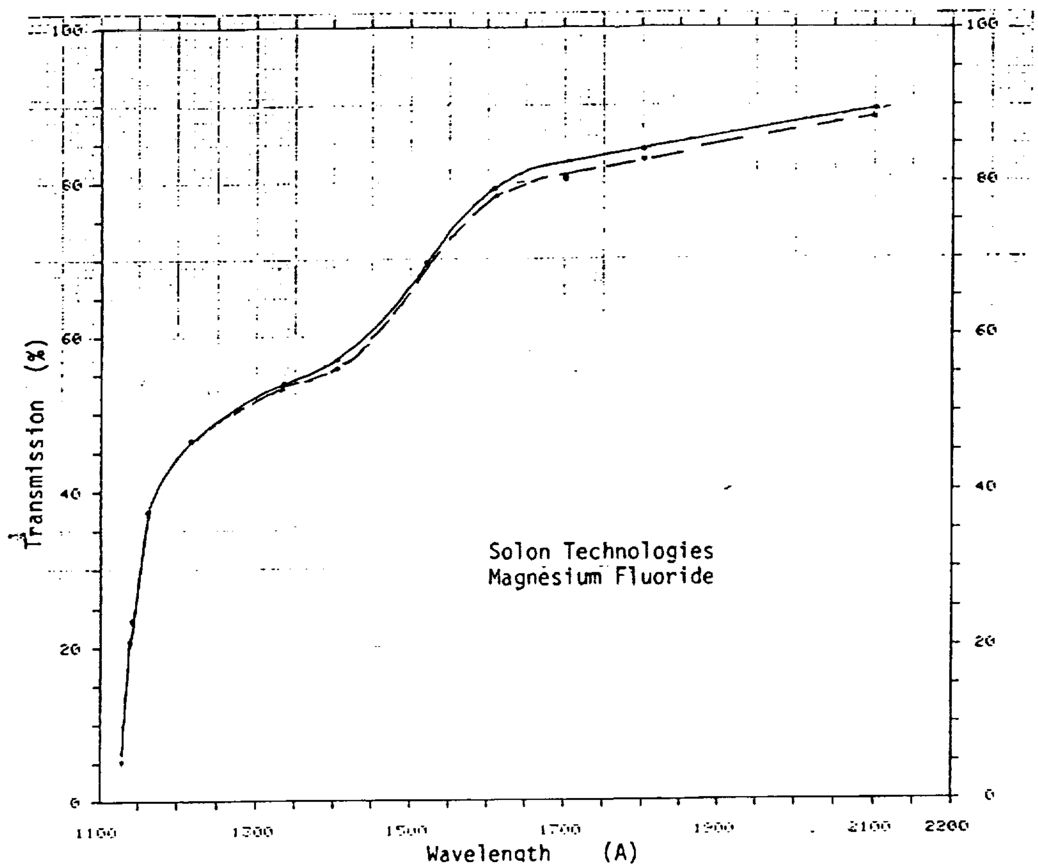
Transmission (%)
Wavelength (A)
Solon Technologies
Magnesium Fluoride

APPENDIX I

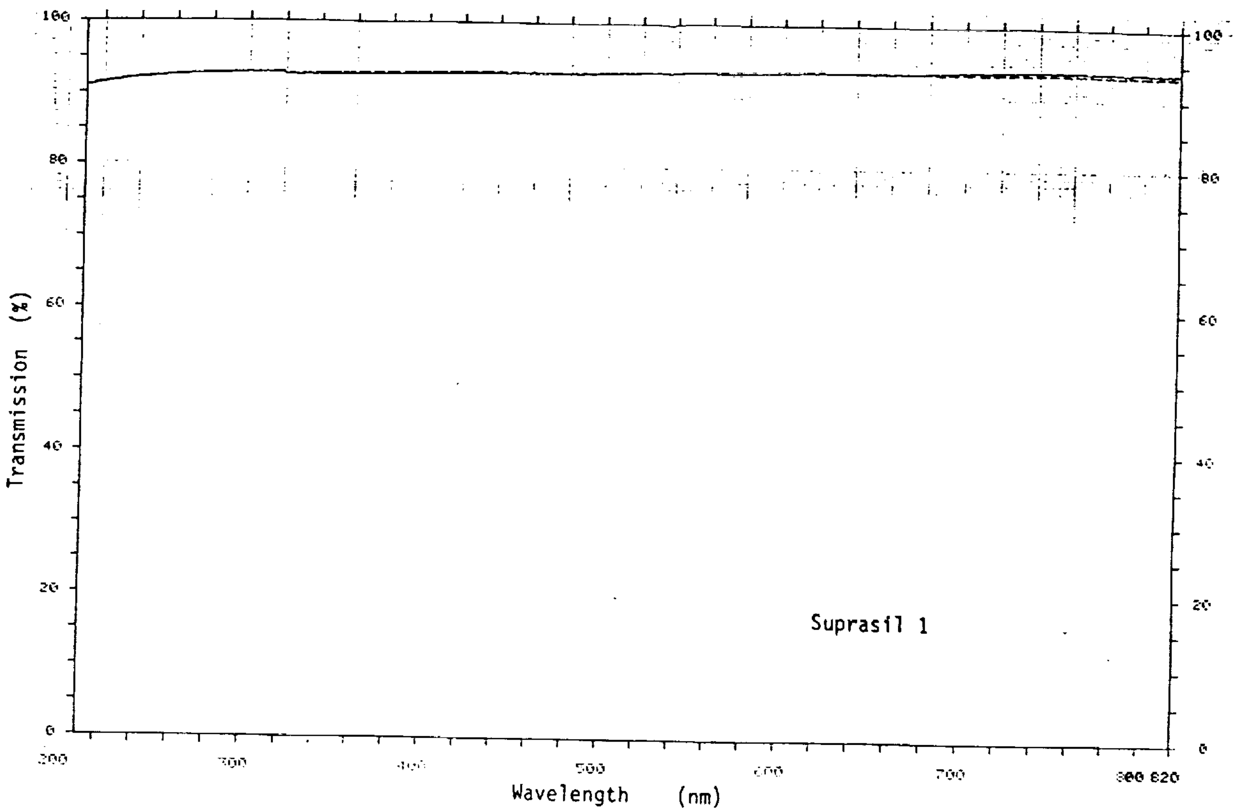
Transmission (%)
Wavelength (nm)
Suprasil 1
100
80
60
40
20
0
200
500
800 820

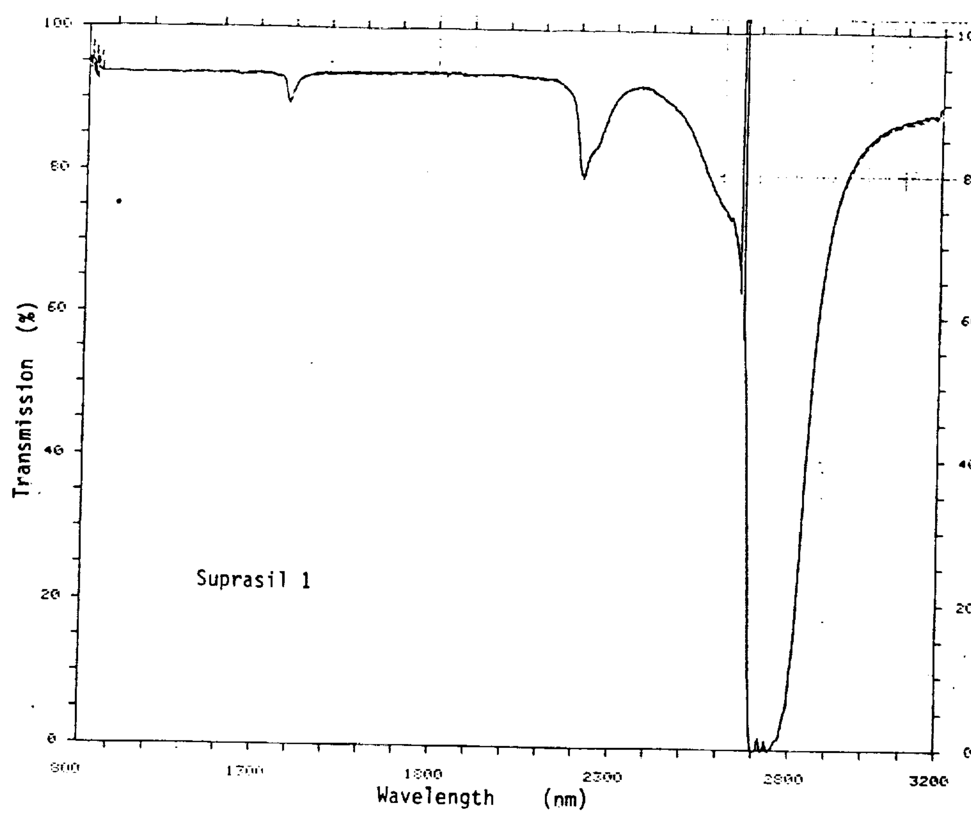
Transmission (%)
Wavelength (nm)
Suprasil 1
100
80
60
40
20
0
1800
2300
2800
3200

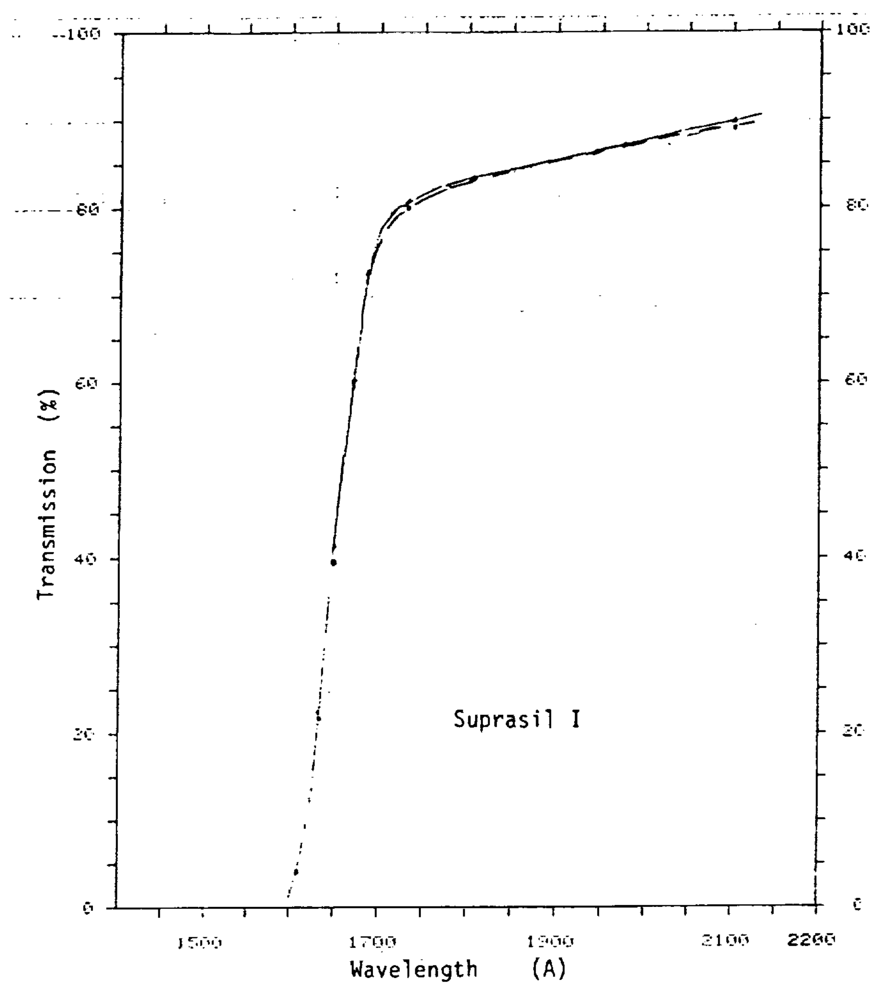

100
80
60
40
20
0
Transmission (%)
Suprasil I
1500
1700
1900
2100
2200
Wavelength (A)

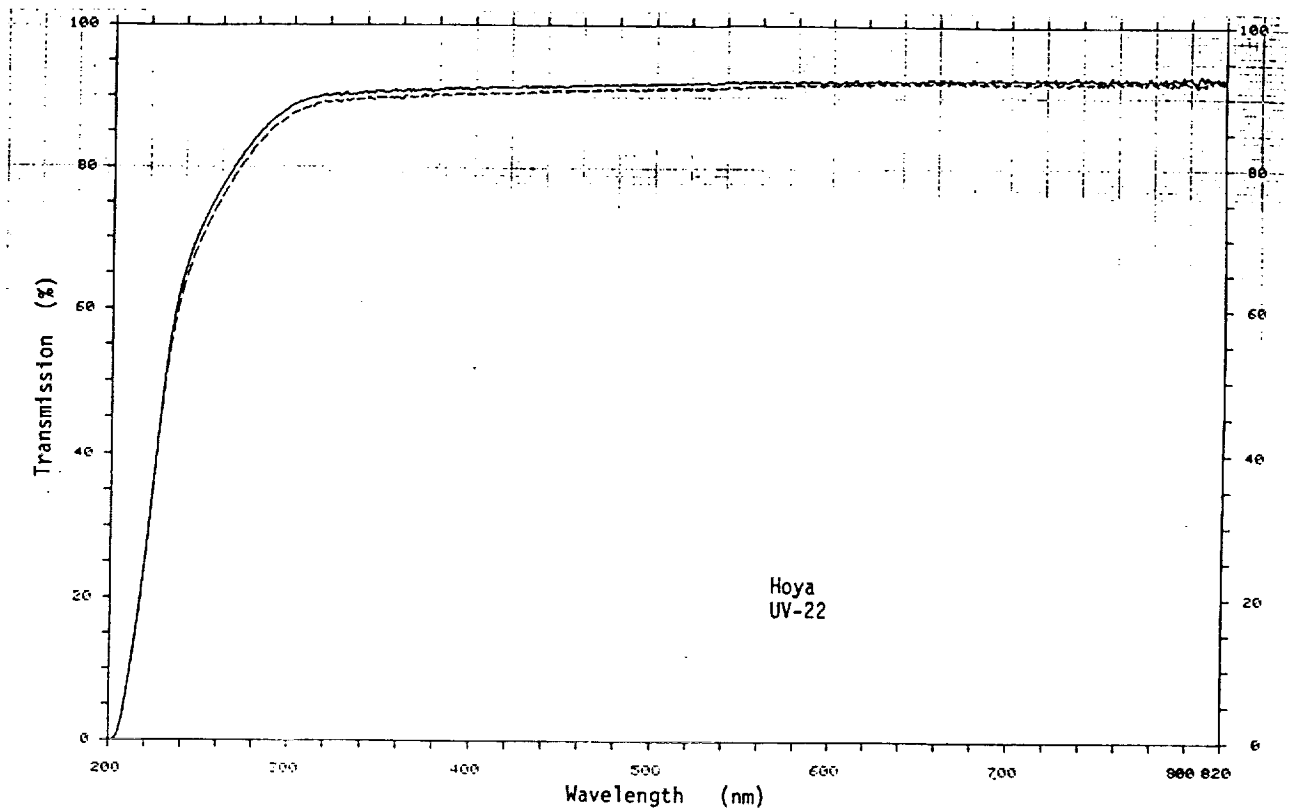

Transmission (%)
Wavelength (nm)
Hoya
UV-22

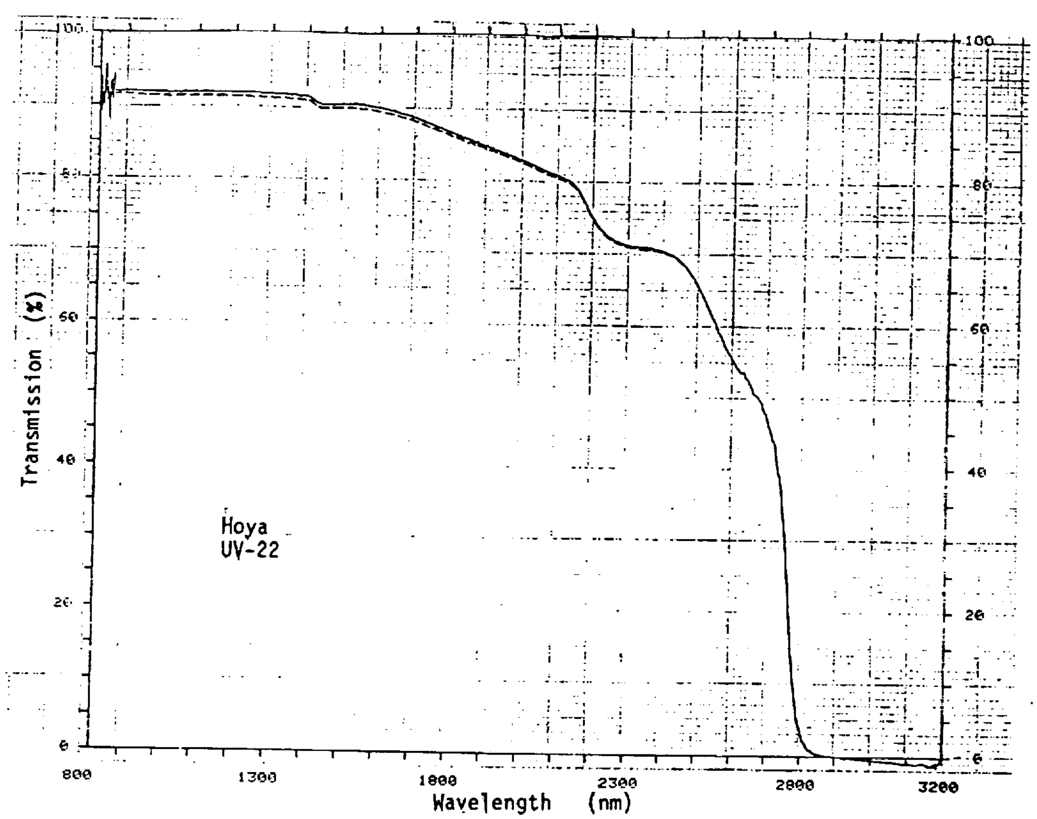

Transmission (%)
Wavelength (nm)
Hoya
UV-22

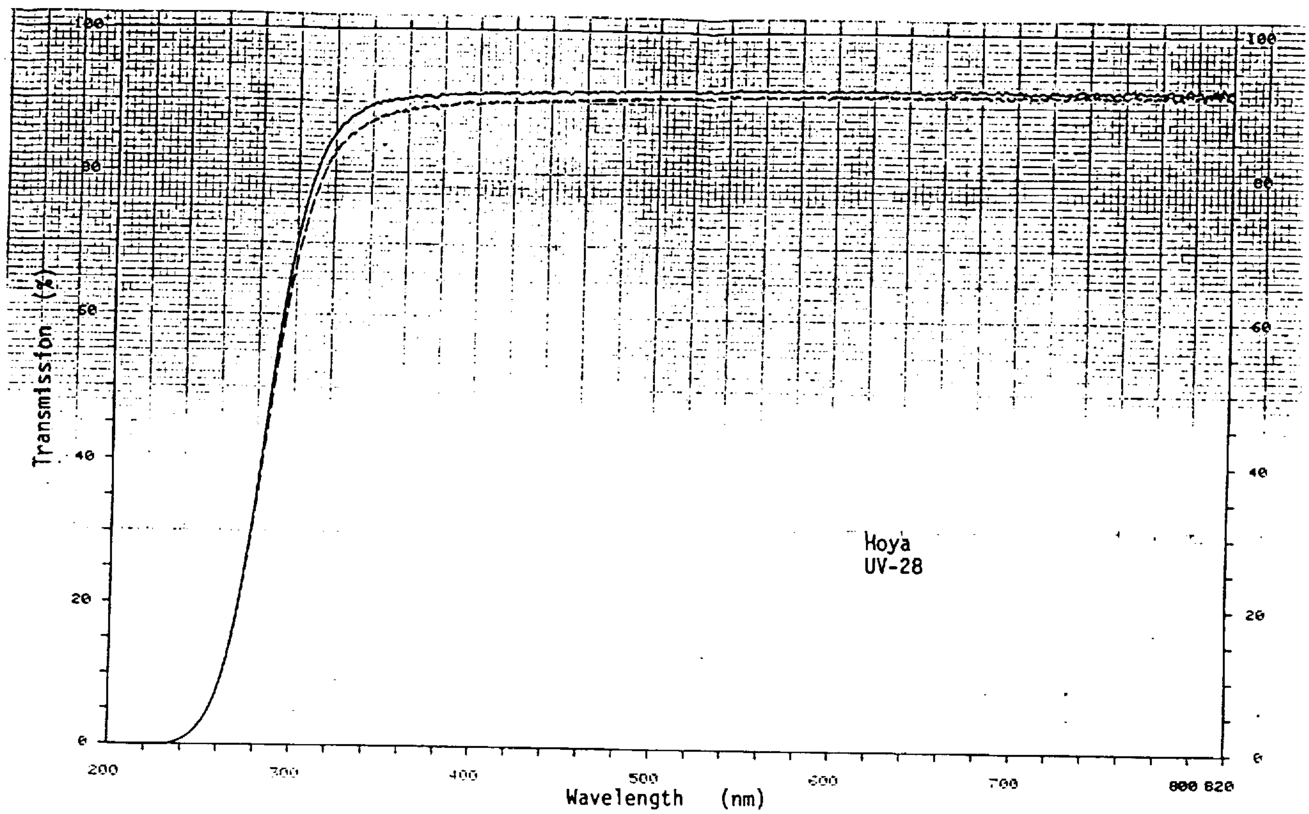
Transmission (%)
Wavelength (nm)
Hoya
UV-28
200
300
400
500
600
700
800 820

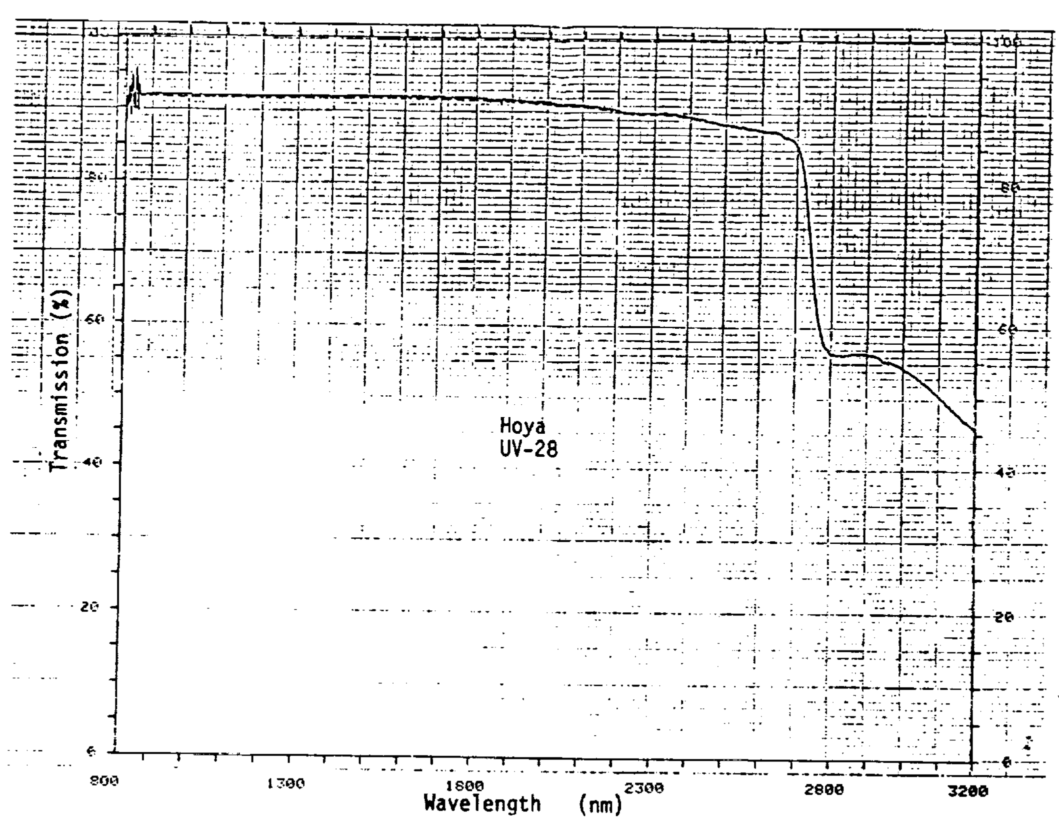
Transmission (%)
Wavelength (nm)
Hoya
UV-28
800
1300
1800
2300
2800
3200

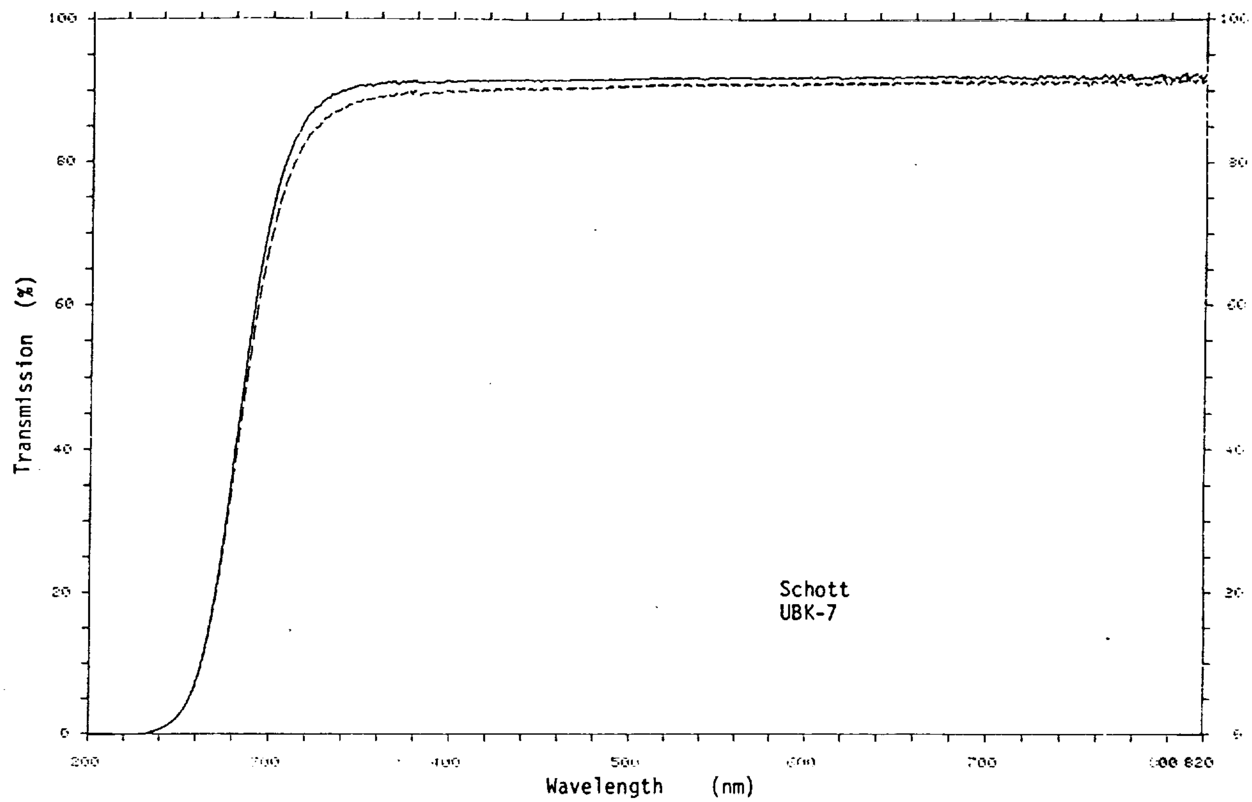
Transmission (%)
Wavelength (nm)
Schott
UBK-7

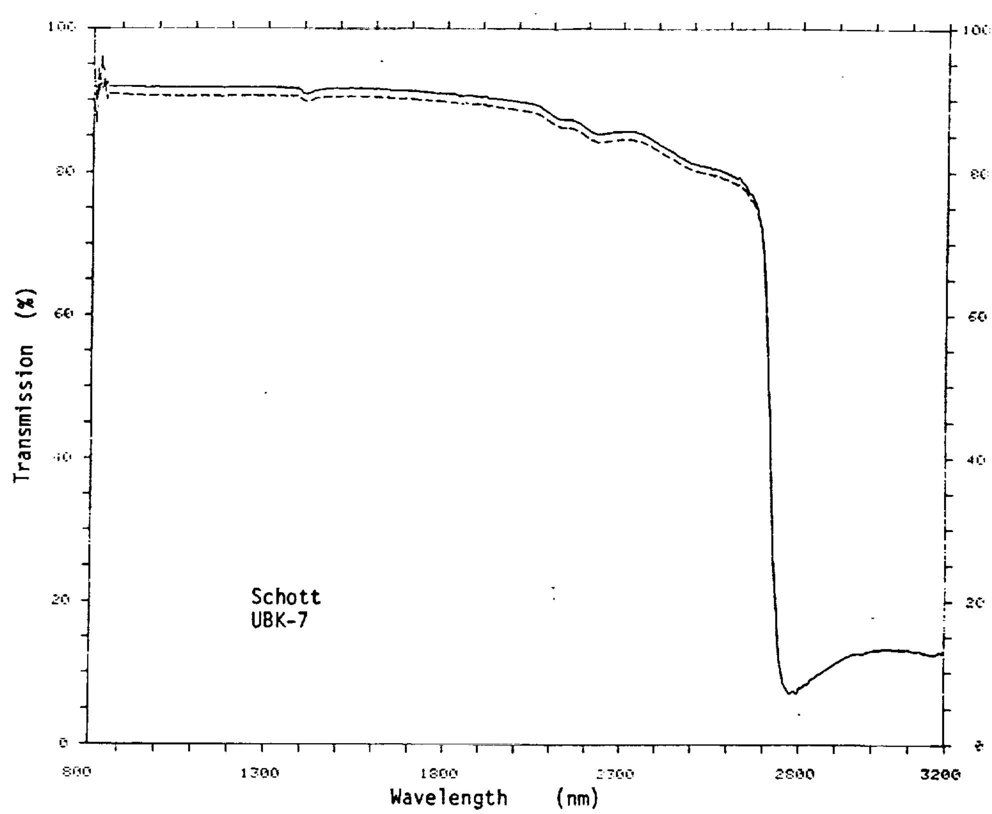
Transmission (%)
Wavelength (nm)
Schott
UBK-7
800
1300
1800
2800
3200

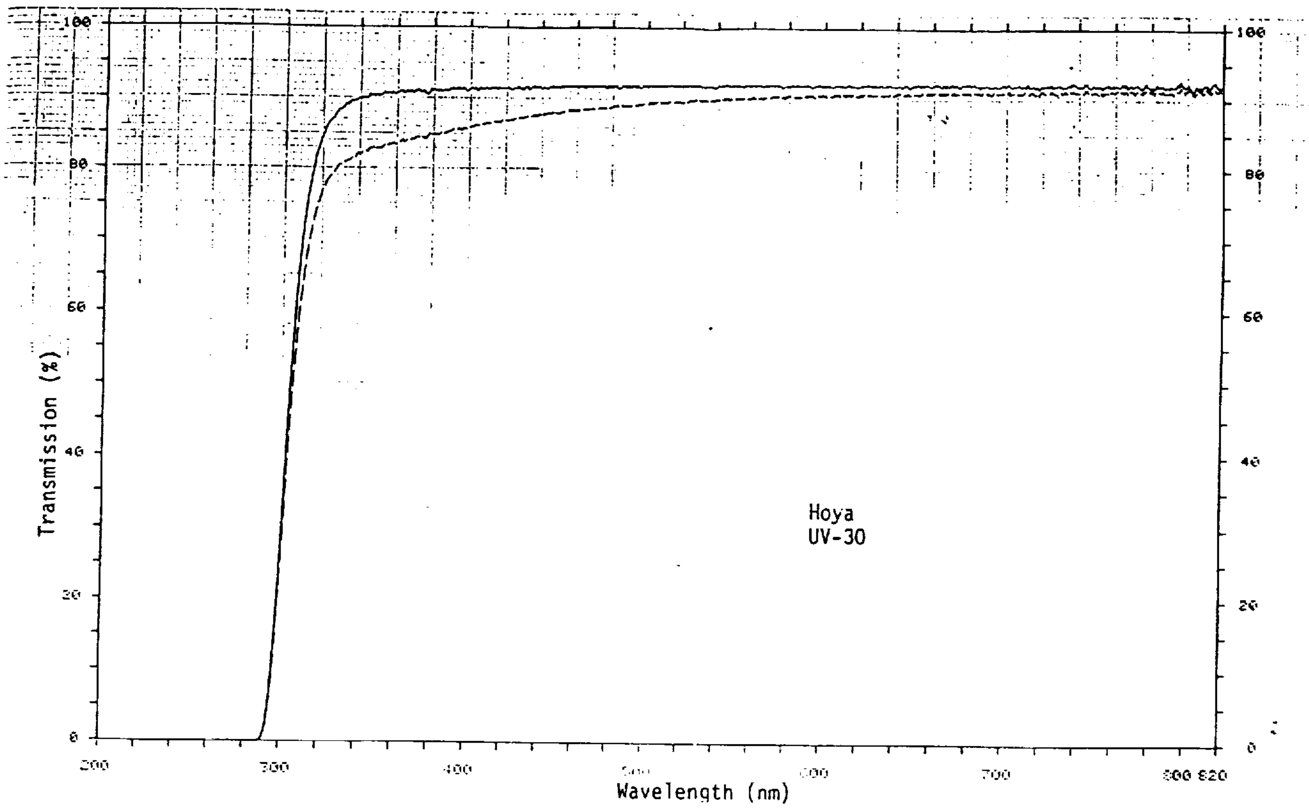
Transmission (%)
Wavelength (nm)
Hoya
UV-30

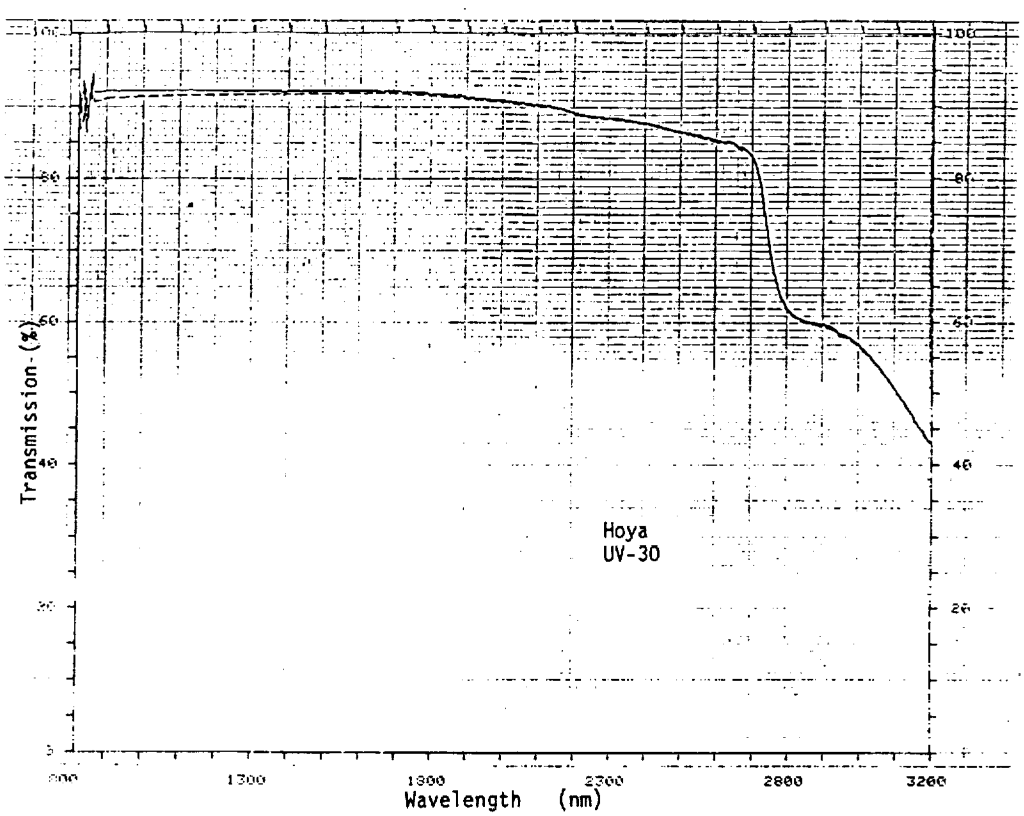
Transmission (%)
Wavelength (nm)
Hoya
UV-30

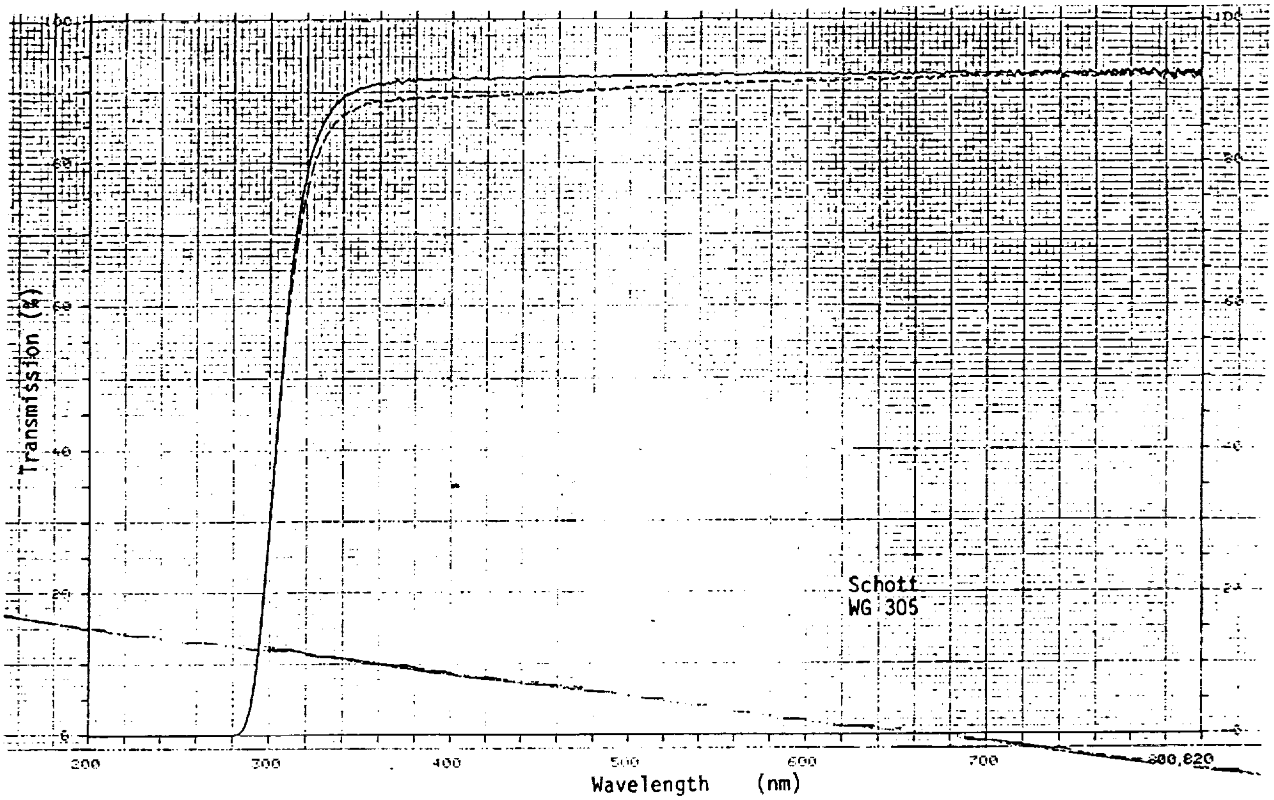

Transmission (%)
Schott
WG 305
Wavelength (nm)

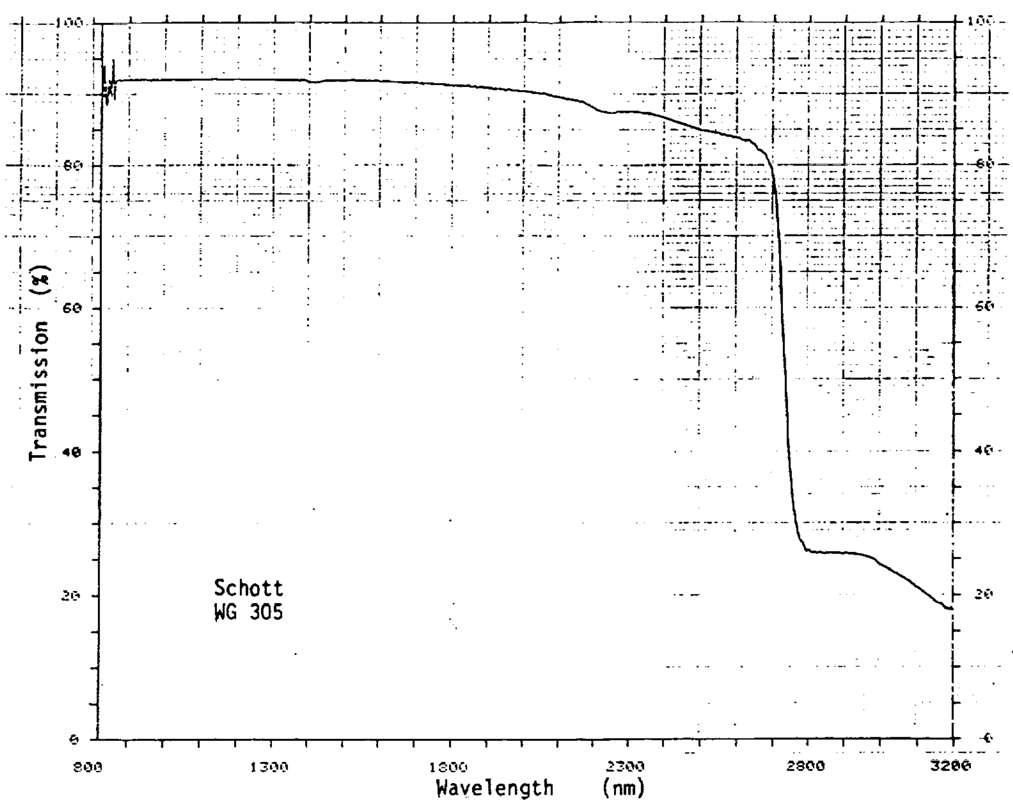

Transmission (%)
Schott
WG 305
Wavelength (nm)

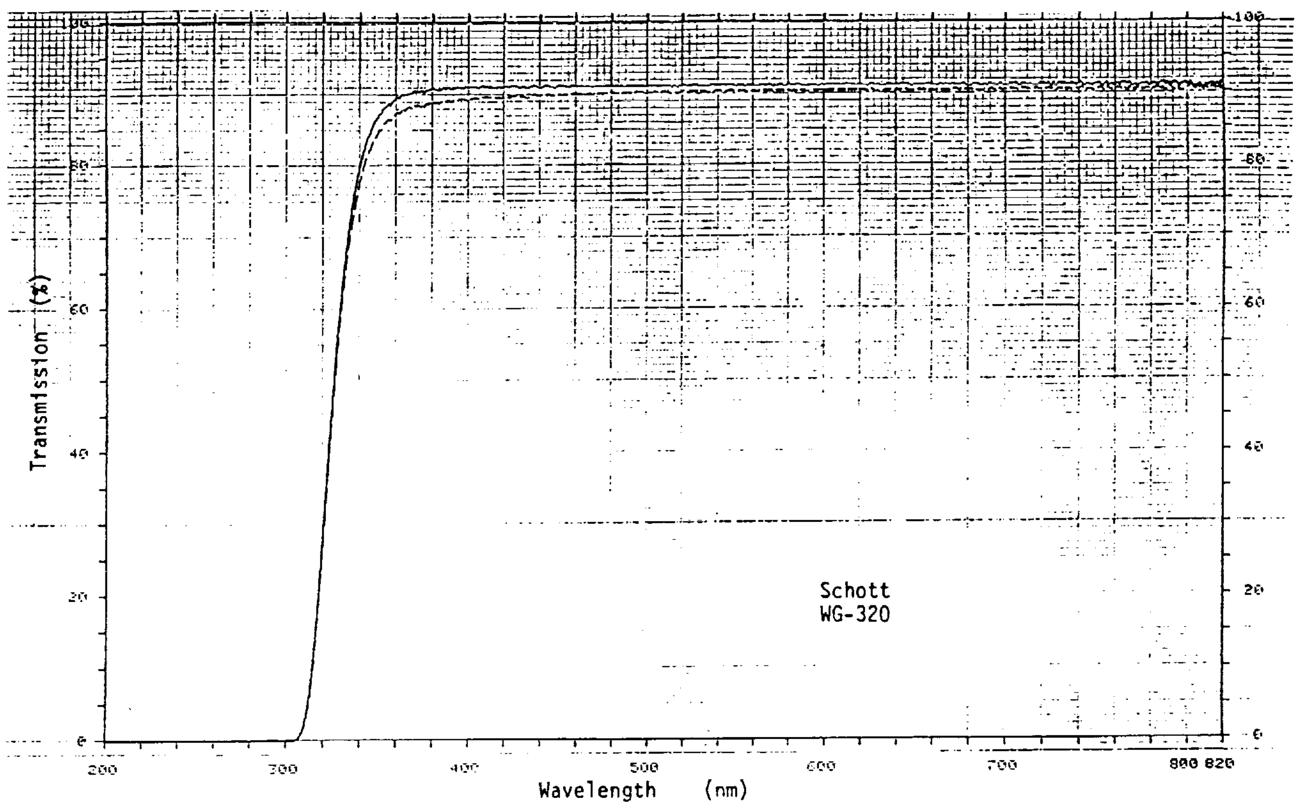

Transmission (%)
Wavelength (nm)
Schott
WG-320

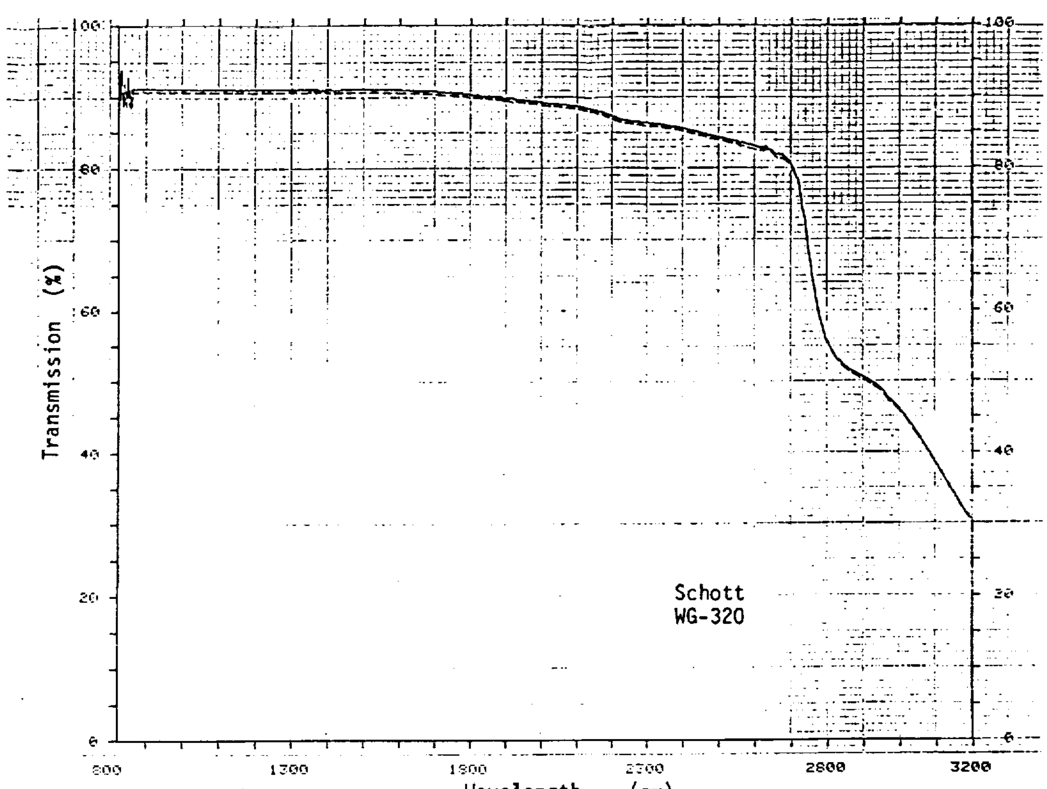

Transmission (%)
Wavelength (nm)
Schott
WG-320

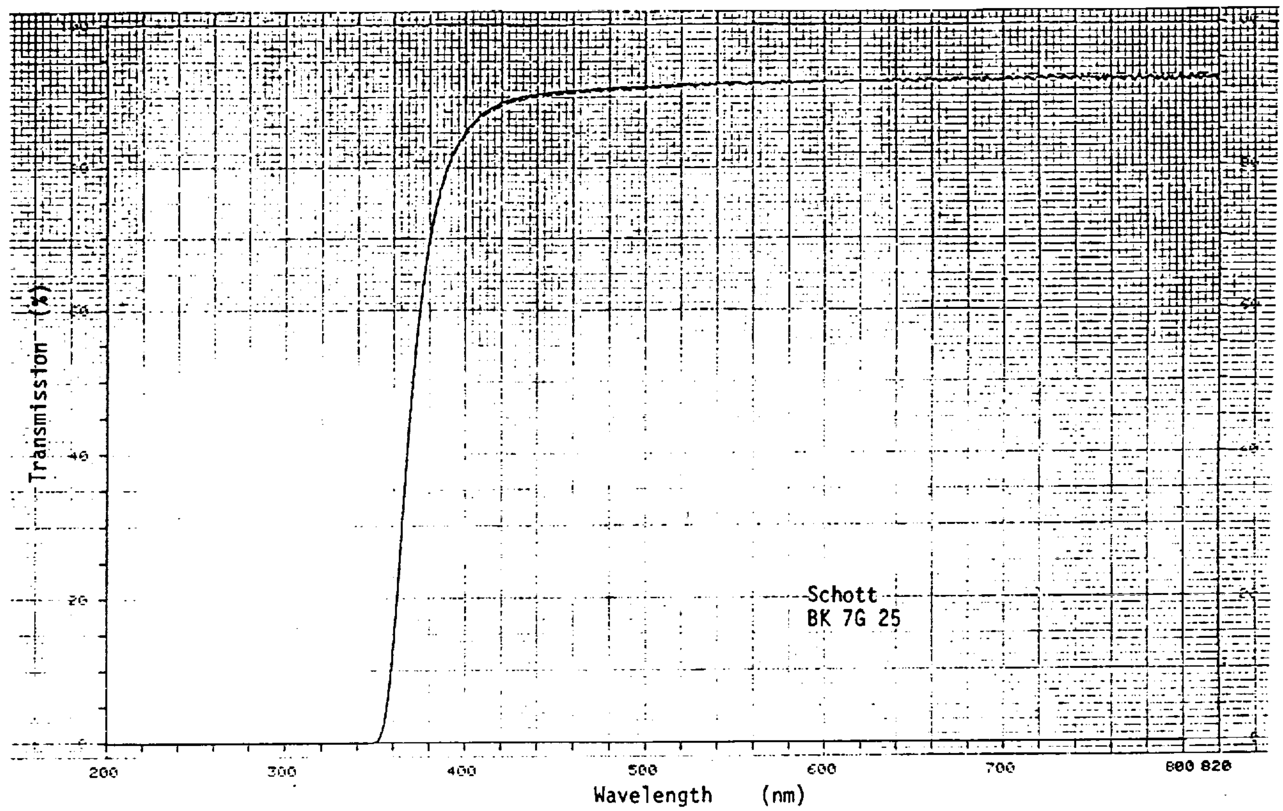
Transmission (%)
20
40
200
300
400
500
600
700
800 820
Wavelength (nm)
Schott
BK 7G 25

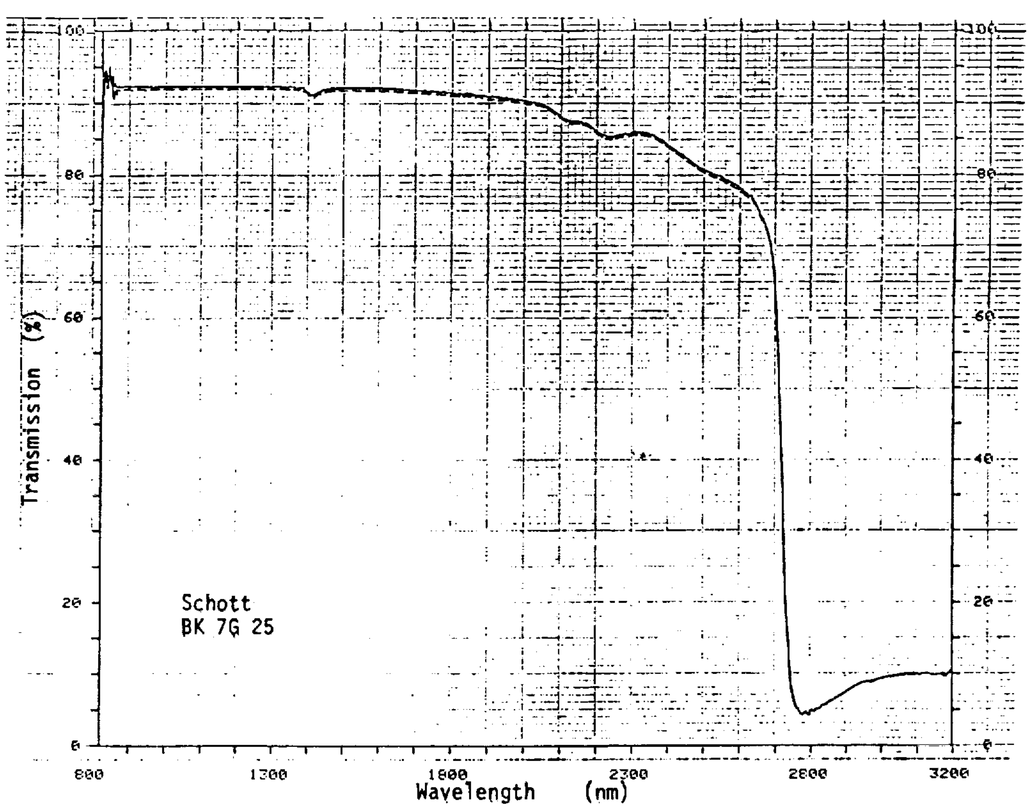
Transmission (%)
100
80
60
40
20
0
800
1300
1800
2300
2800
3200
Wavelength (nm)
Schott
BK 7G 25

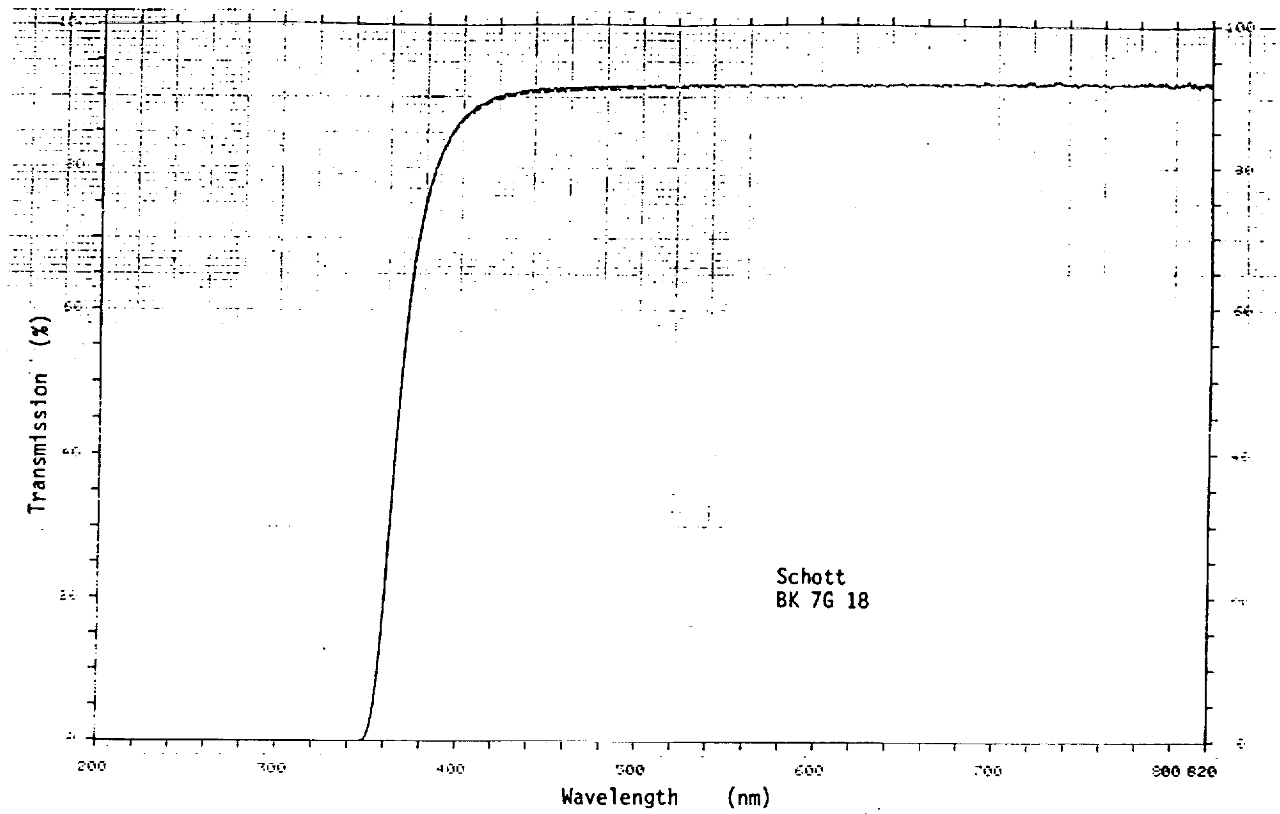
Transmission (%)
Schott
BK 7G 18
200
300
400
500
600
700
800 820
Wavelength (nm)

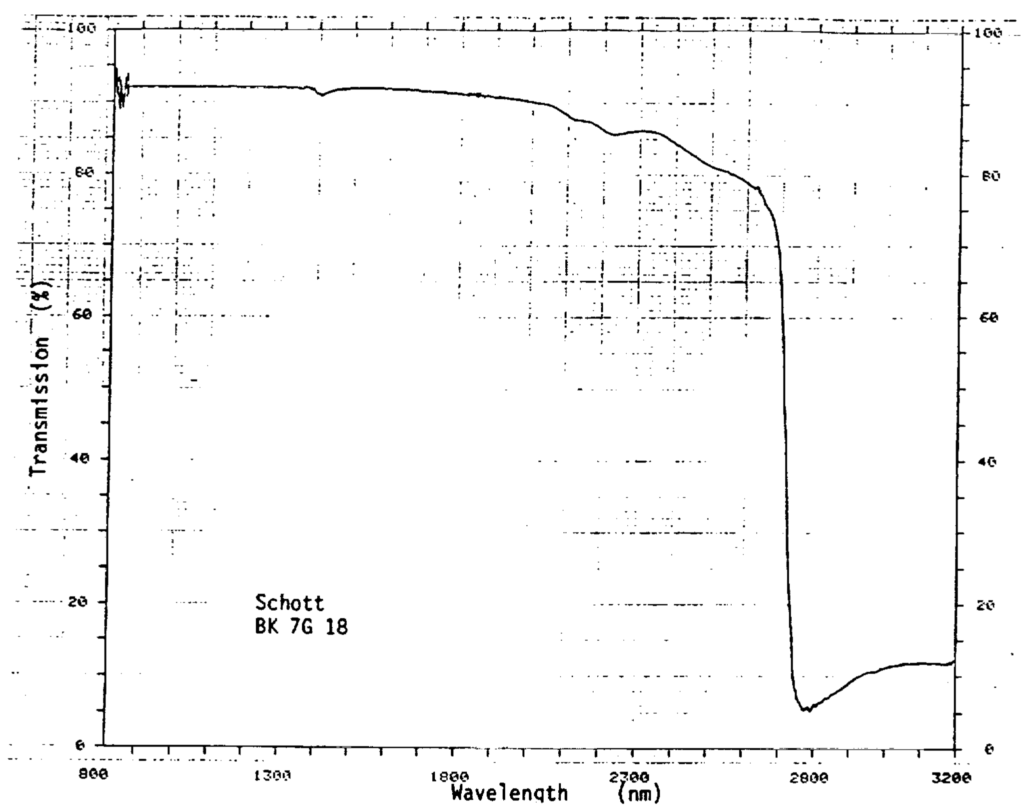
100
80
60
40
20
0
Transmission (%)
Schott
BK 7G 18
800
1300
1800
2300
2800
3200
Wavelength (nm)

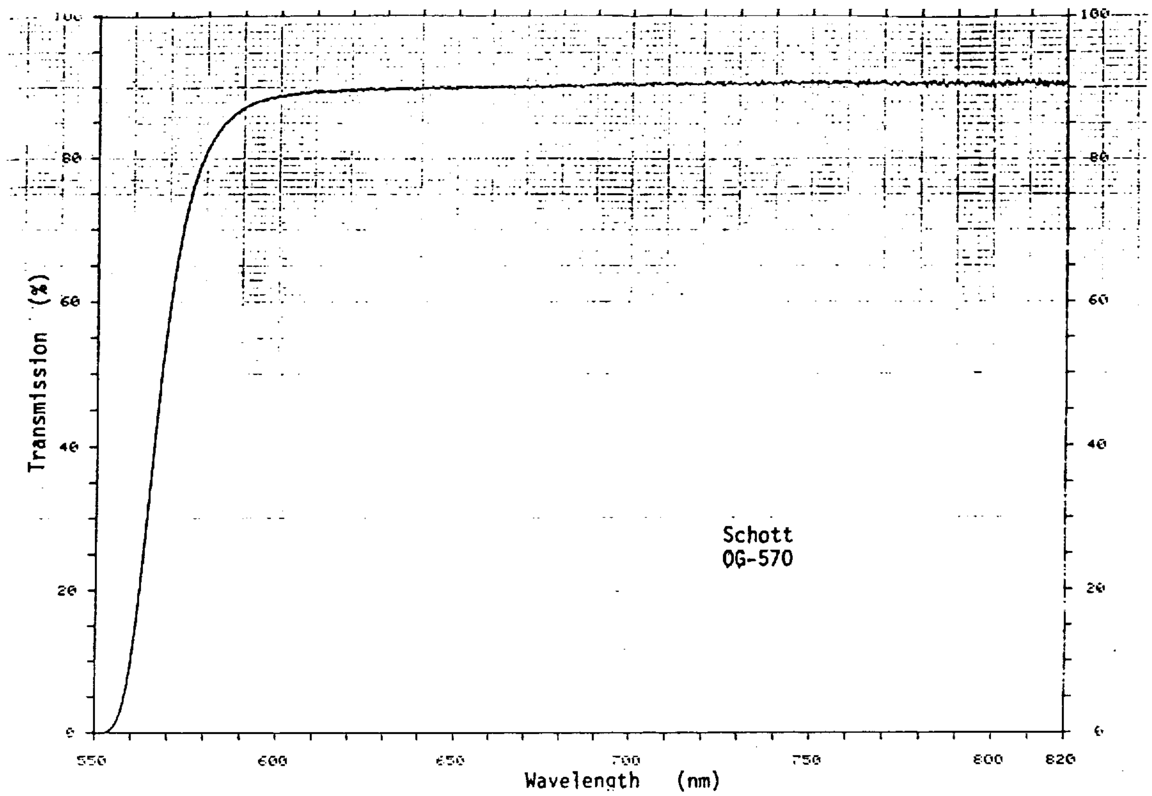
Transmission (%)
Wavelength (nm)
Schott
OG-570
550
600
650
700
750
800
820

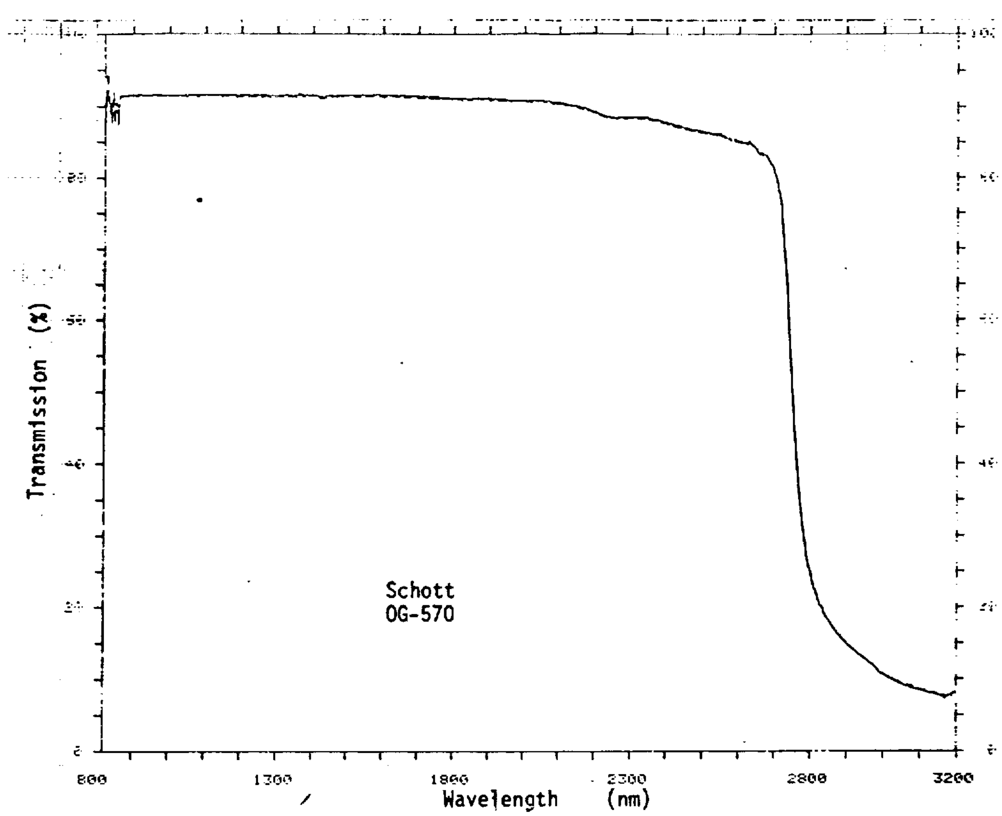
Transmission (%)
Wavelength (nm)
Schott
OG-570
800
1300
1800
2300
2800
3200

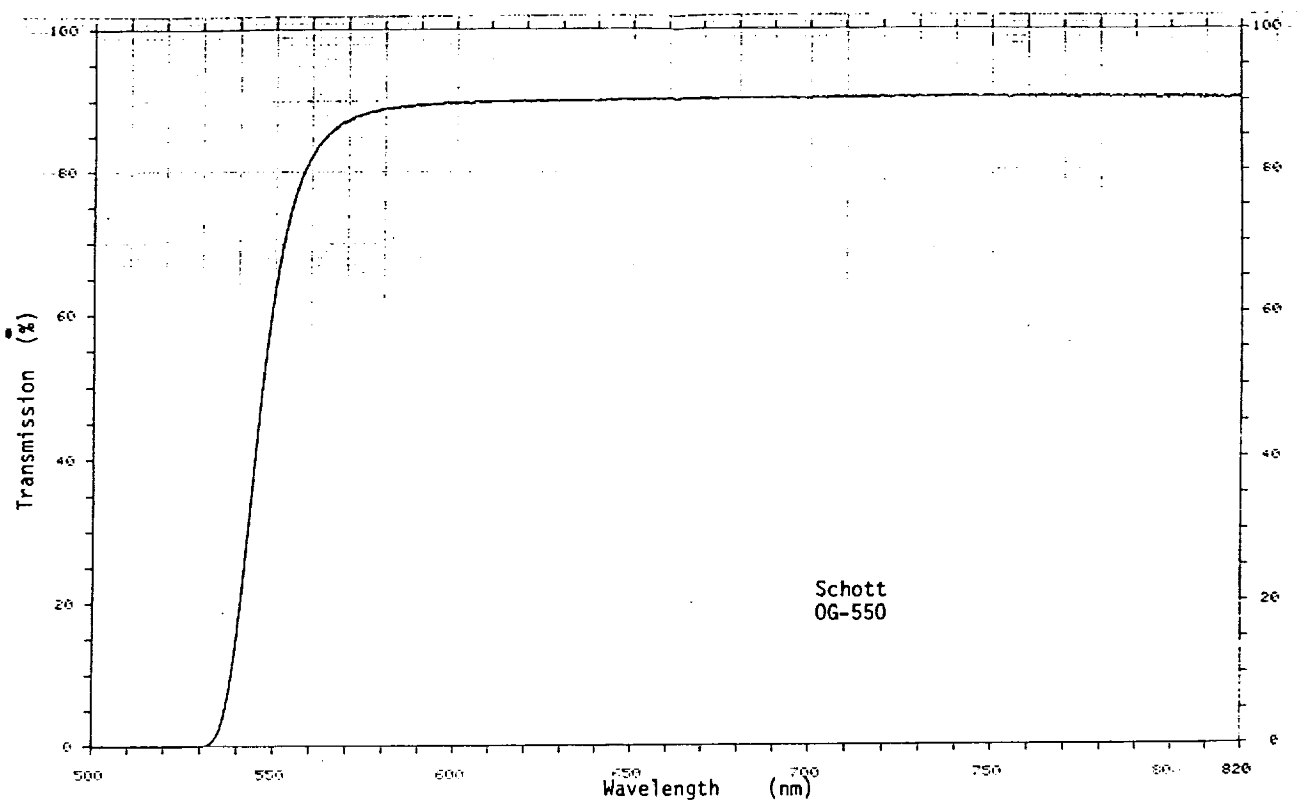
Transmission (%)
Wavelength (nm)
Schott
OG-550

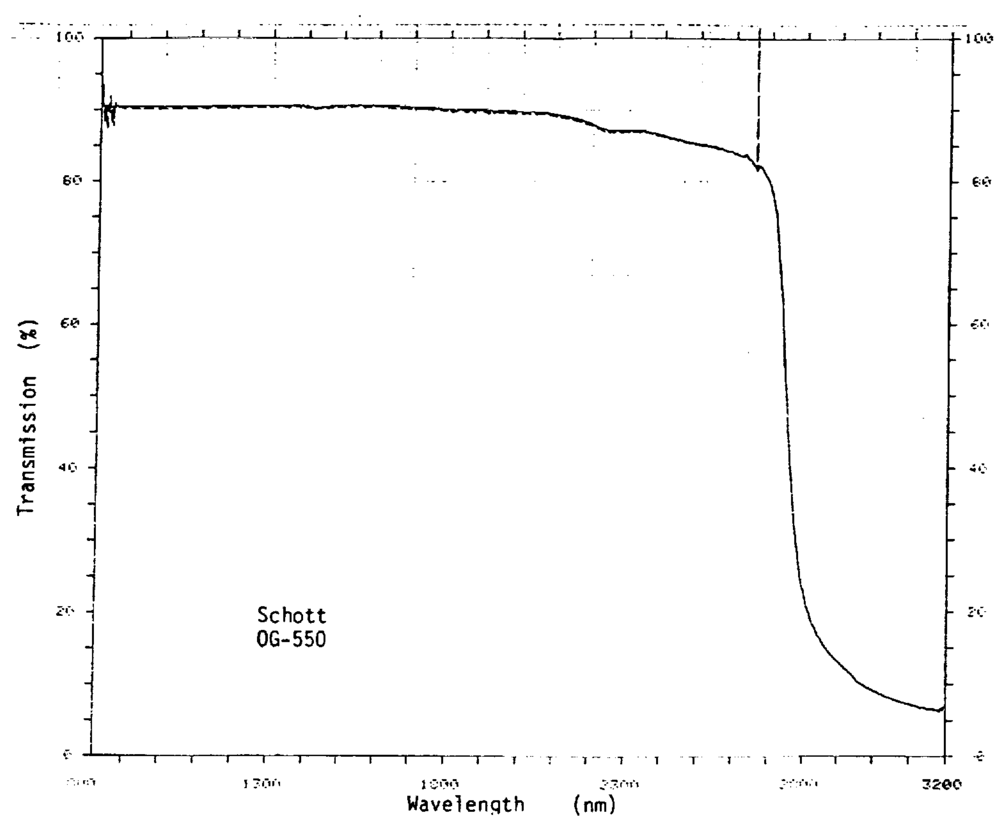
Transmission (%)
Wavelength (nm)
Schott
OG-550

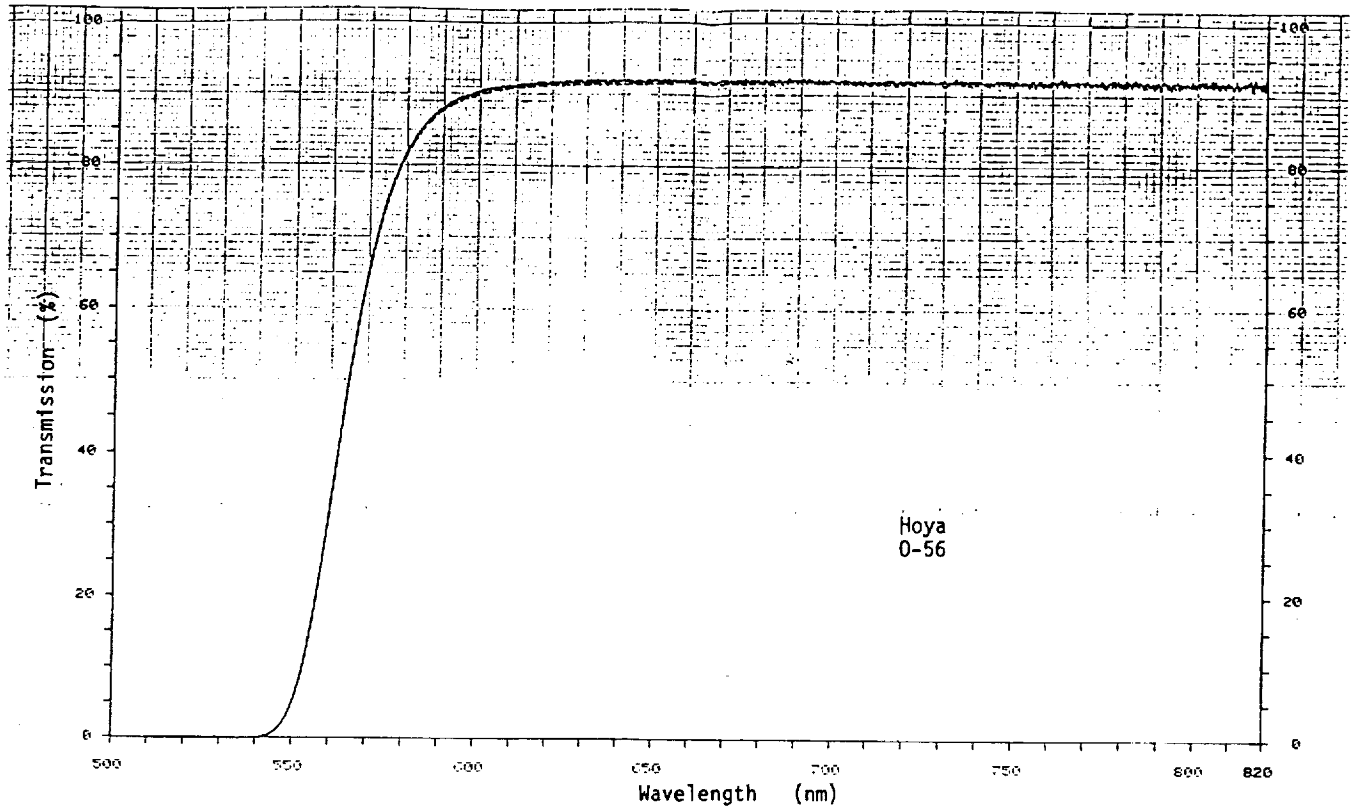
Transmission (%)
Wavelength (nm)
Hoya
O-56
100
80
60
40
20
0
500
550
600
650
700
750
800
820

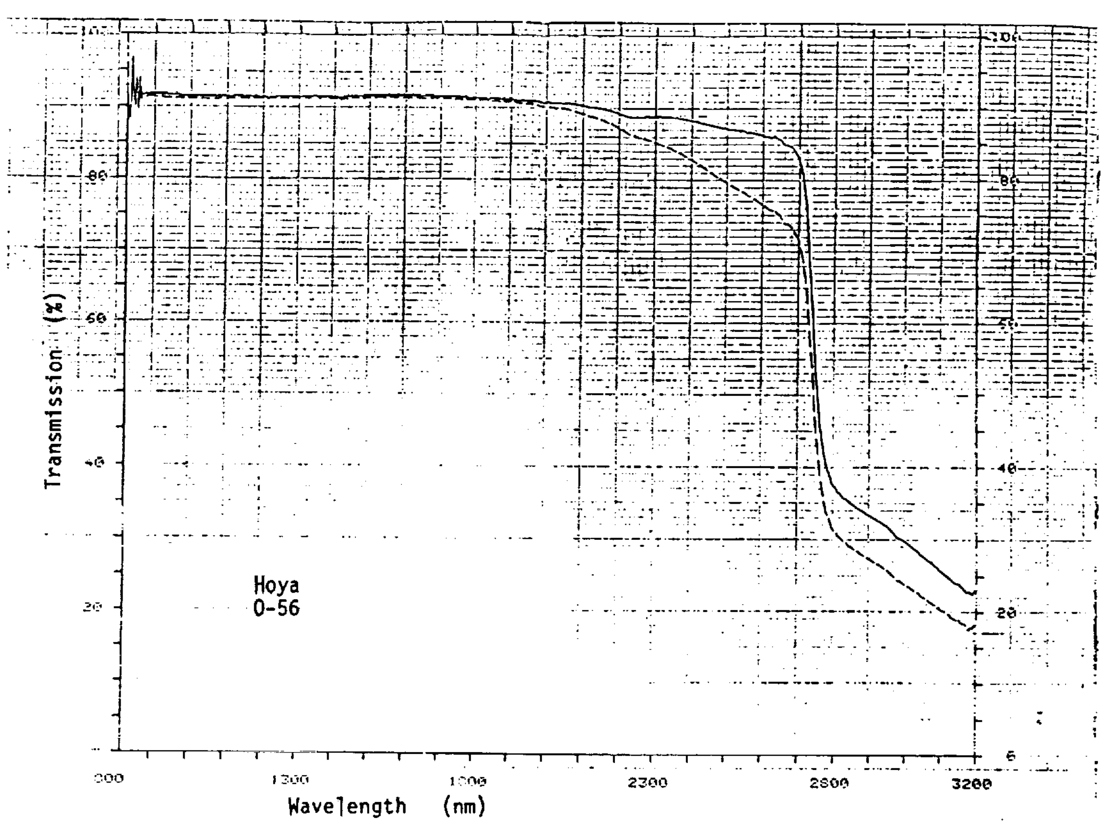
Transmission (%)
Wavelength (nm)
Hoya
O-56
80
60
40
20
2300
2800
3200

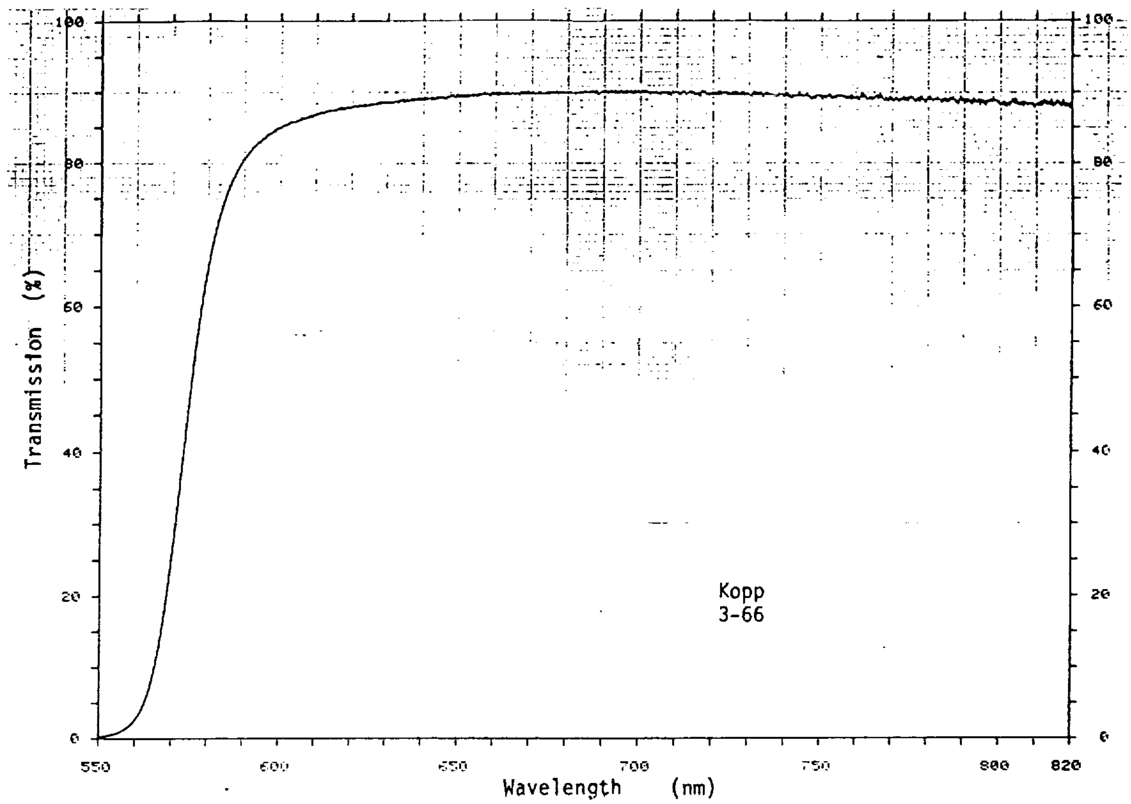
Transmission (%)
Wavelength (nm)
Kopp
3-66
0
20
40
60
80
100
550
600
650
700
750
800
820

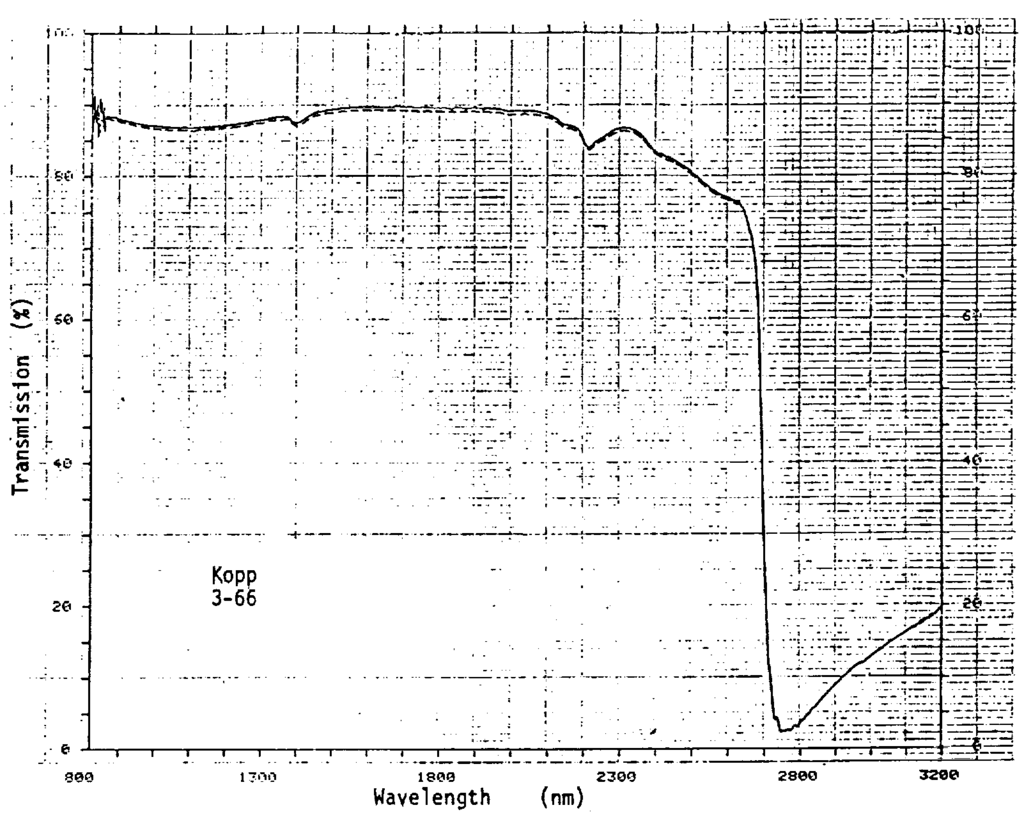
Transmission (%)
Wavelength (nm)
Kopp
3-66
0
20
40
60
80
100
800
1300
1800
2300
2800
3200

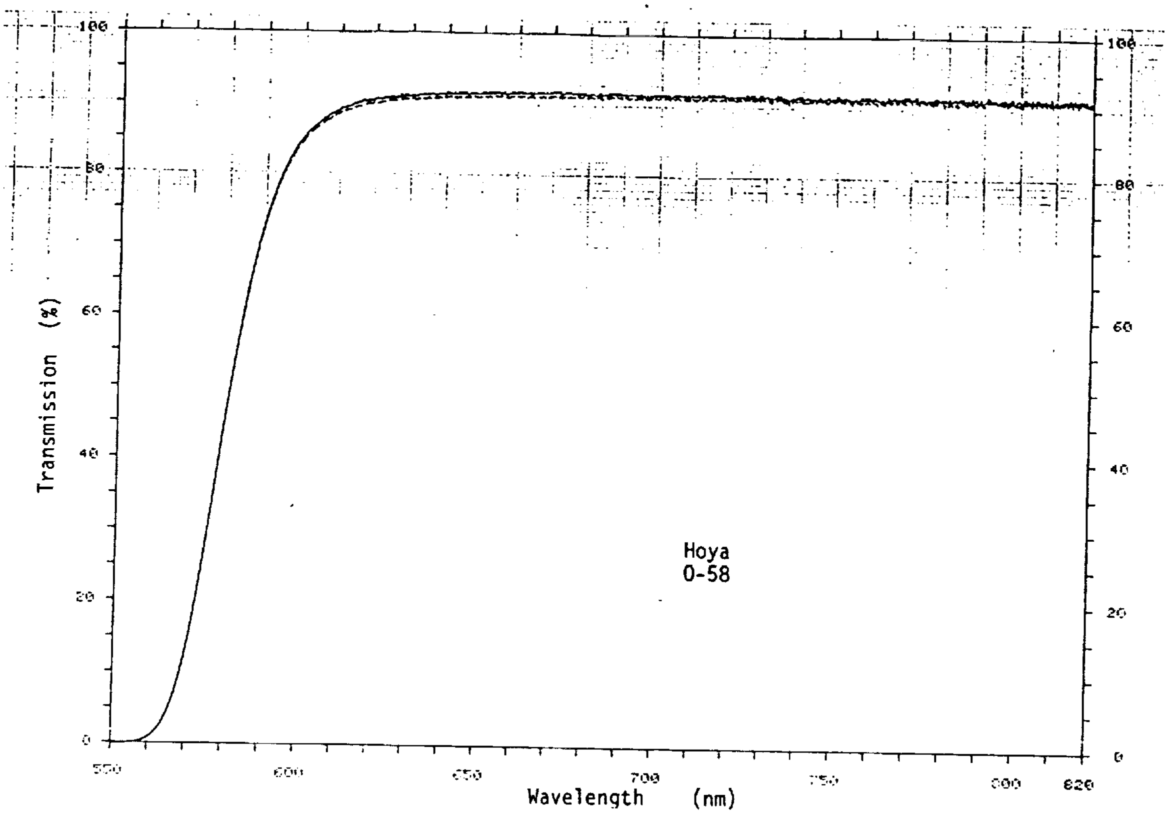
Transmission (%)
Wavelength (nm)
Hoya
O-58

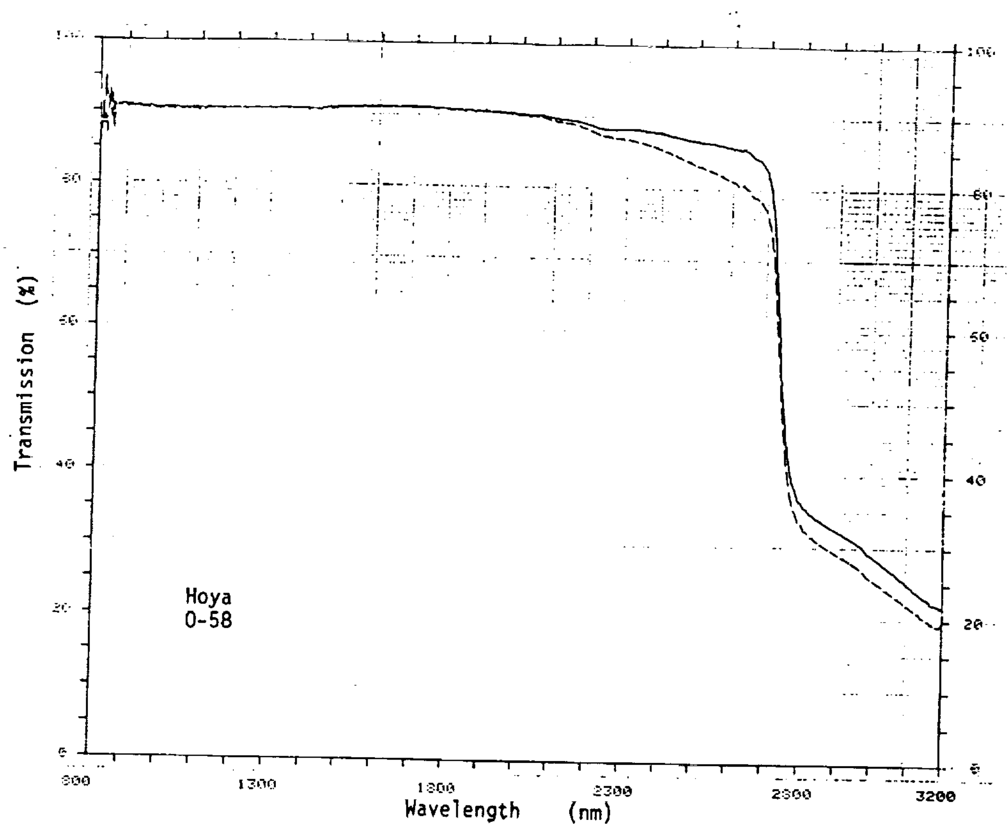
Transmission (%)
Wavelength (nm)
Hoya
O-58

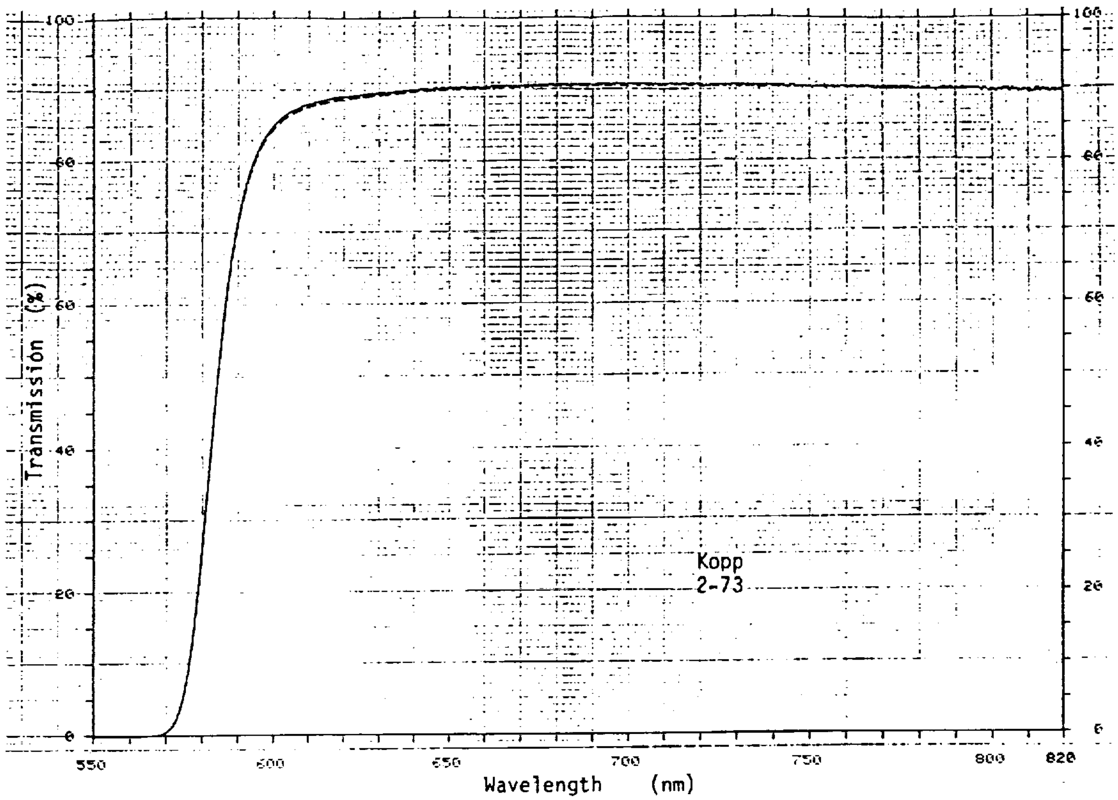
100
80
60
40
20
0
Transmission (%)
Kopp
2-73
550
600
650
700
750
800
820
Wavelength (nm)

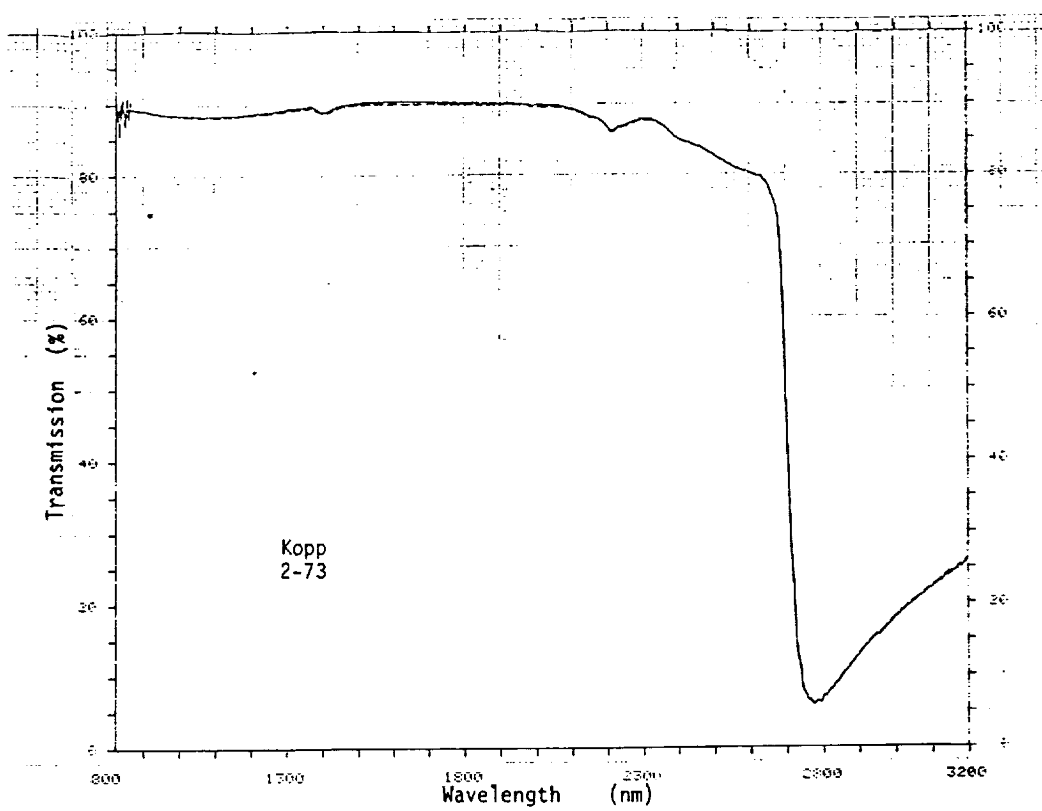
100
80
60
40
20
0
Transmission (%)
Kopp
2-73
800
1300
1800
2300
2800
3200
Wavelength (nm)

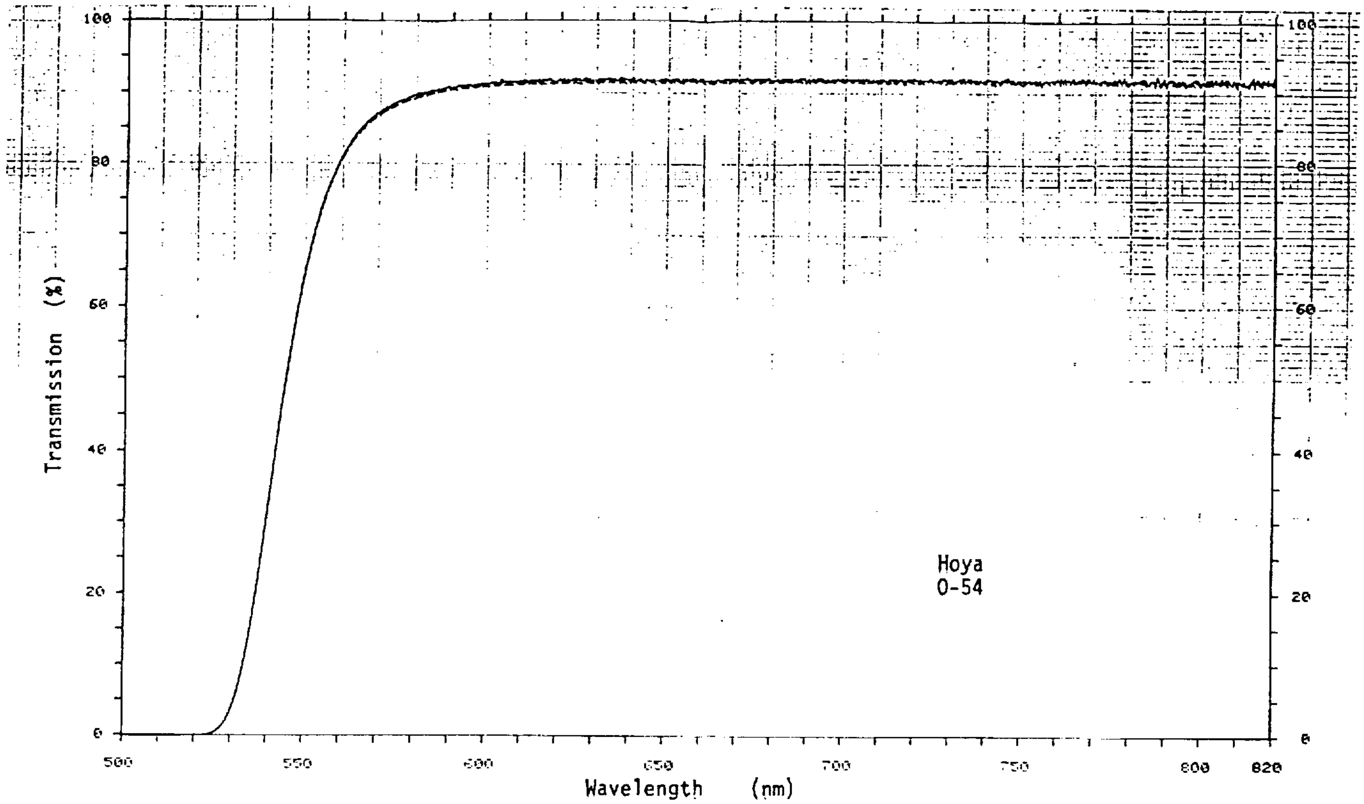
Transmission (%)
0
20
40
60
80
100
500
550
600
650
700
750
800
820
Wavelength (nm)
Hoya
O-54

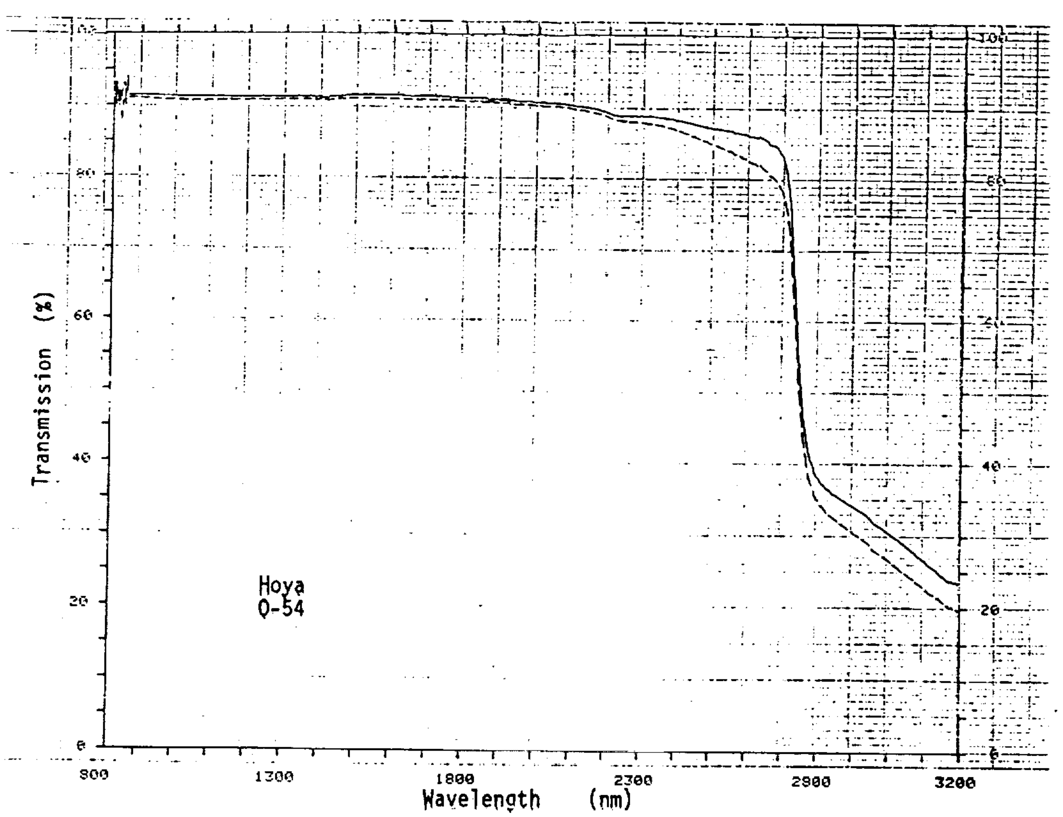
Transmission (%)
0
20
40
60
80
800
1300
1800
2300
2800
3200
Wavelength (nm)
Hoya
O-54

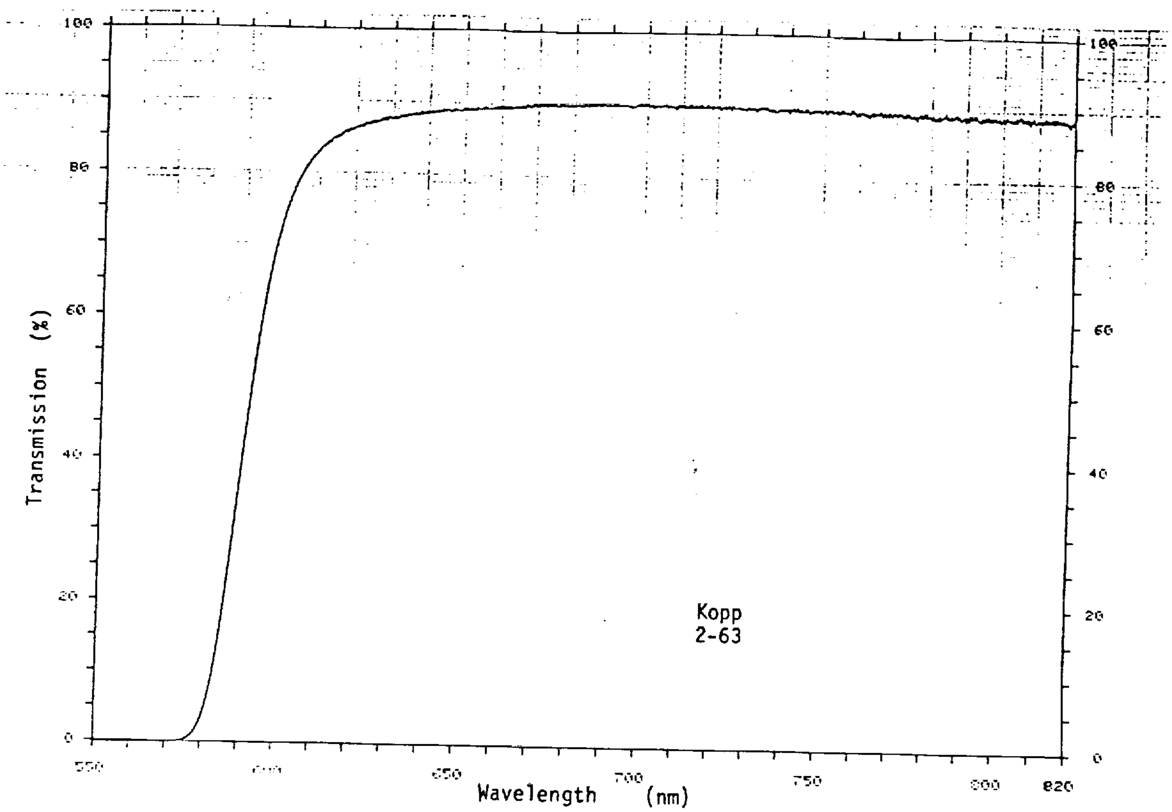
Transmission (%)
Wavelength (nm)
Kopp
2-63

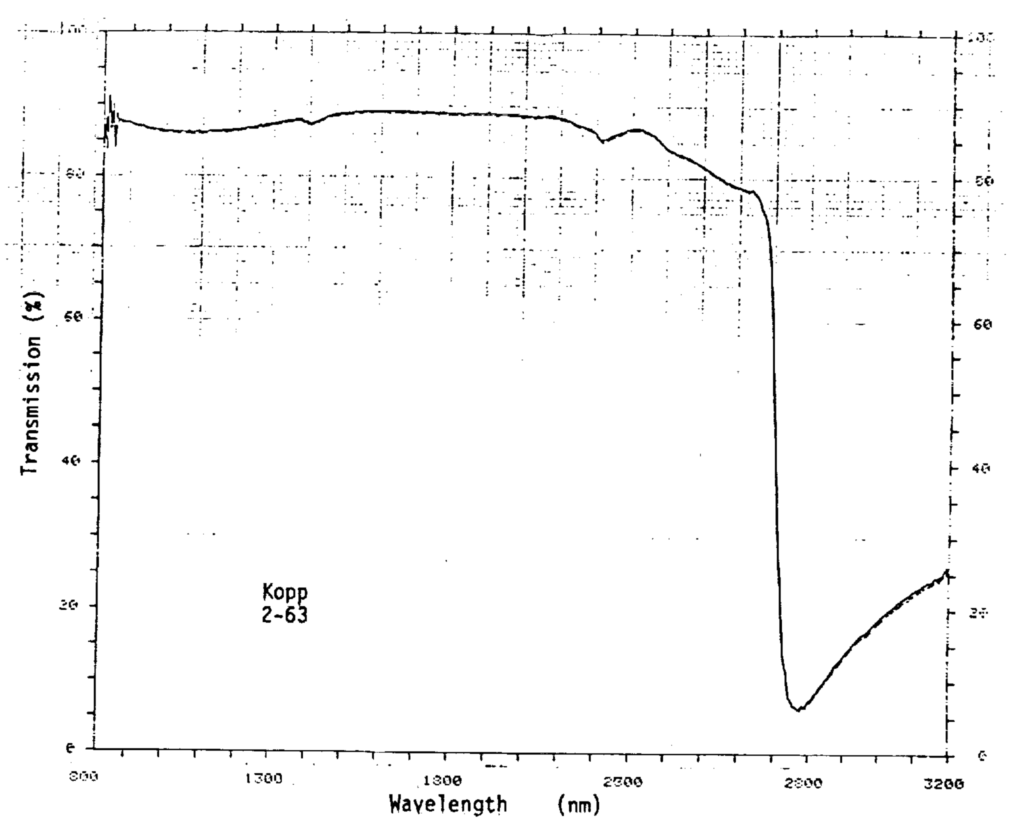
Transmission (%)
Wavelength (nm)
Kopp
2-63

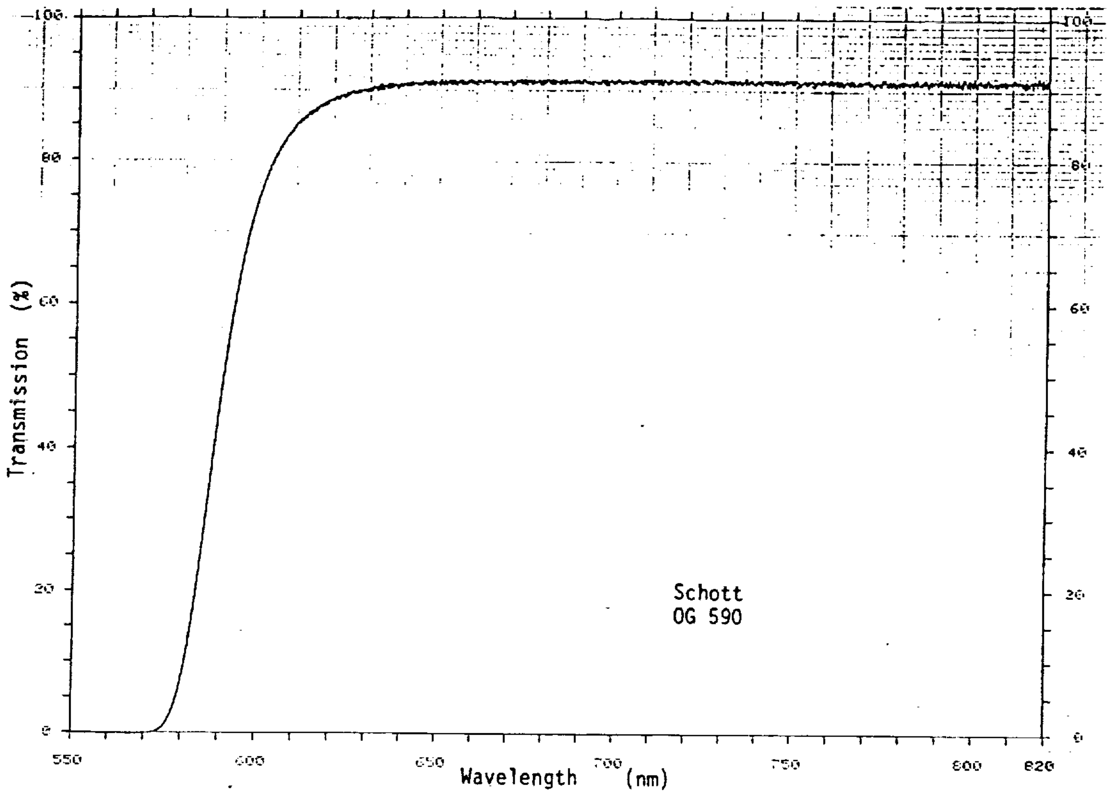
Transmission (%)
Wavelength (nm)
Schott
OG 590

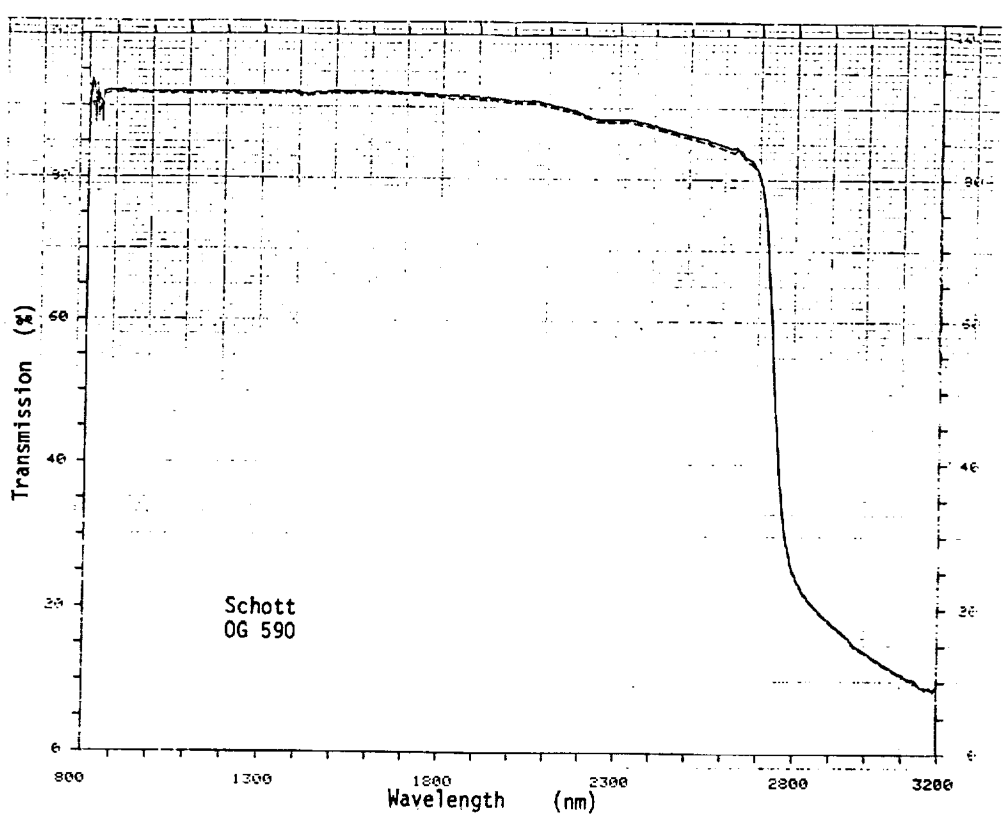
Transmission (%)
Wavelength (nm)
Schott
OG 590

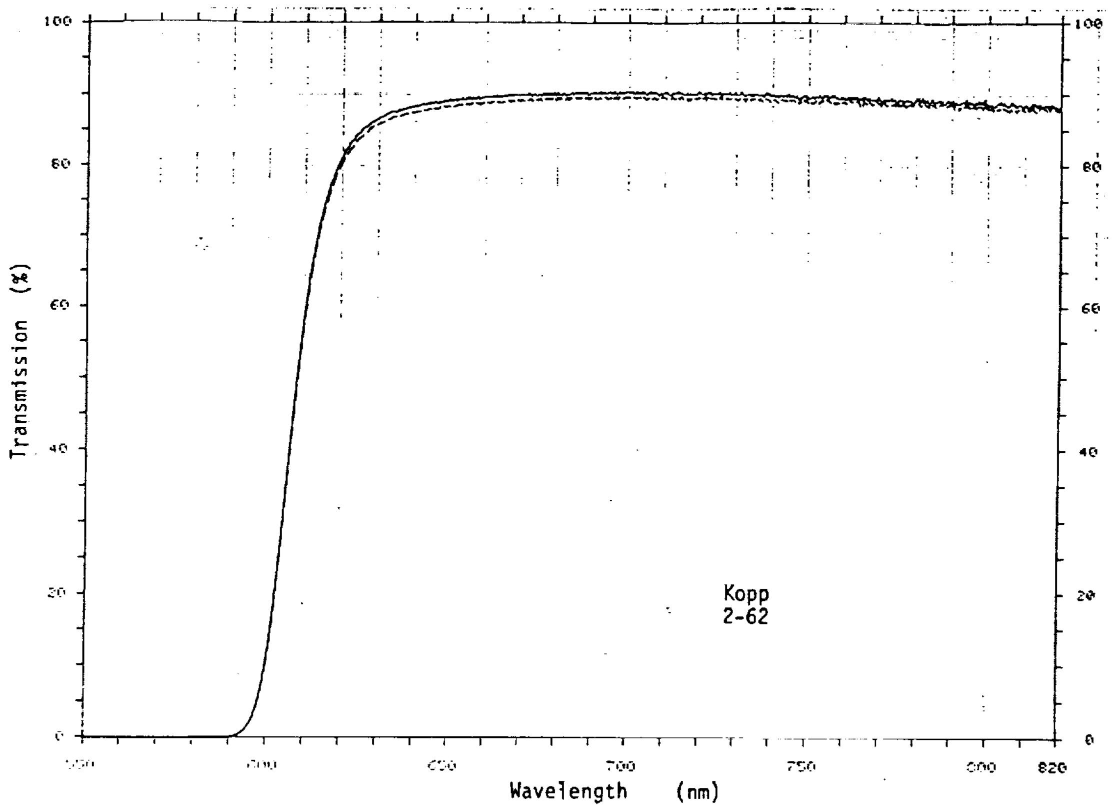
Transmission (%)
Wavelength (nm)
Kopp
2-62

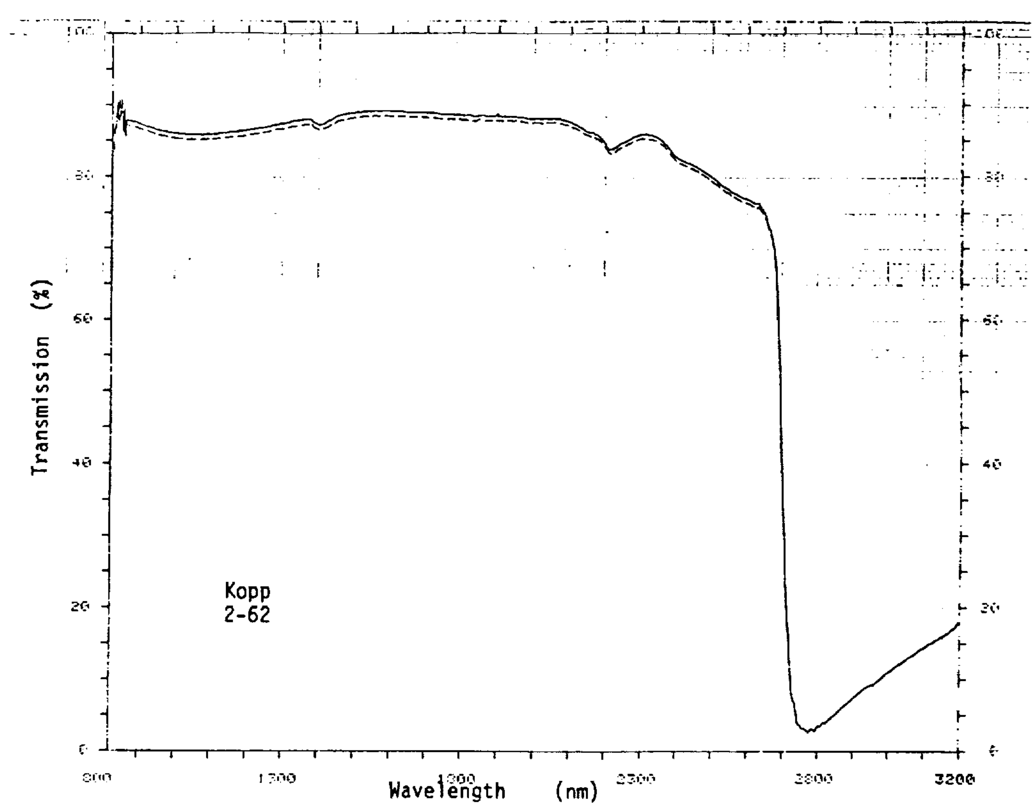
Transmission (%)
Wavelength (nm)
Kopp
2-62

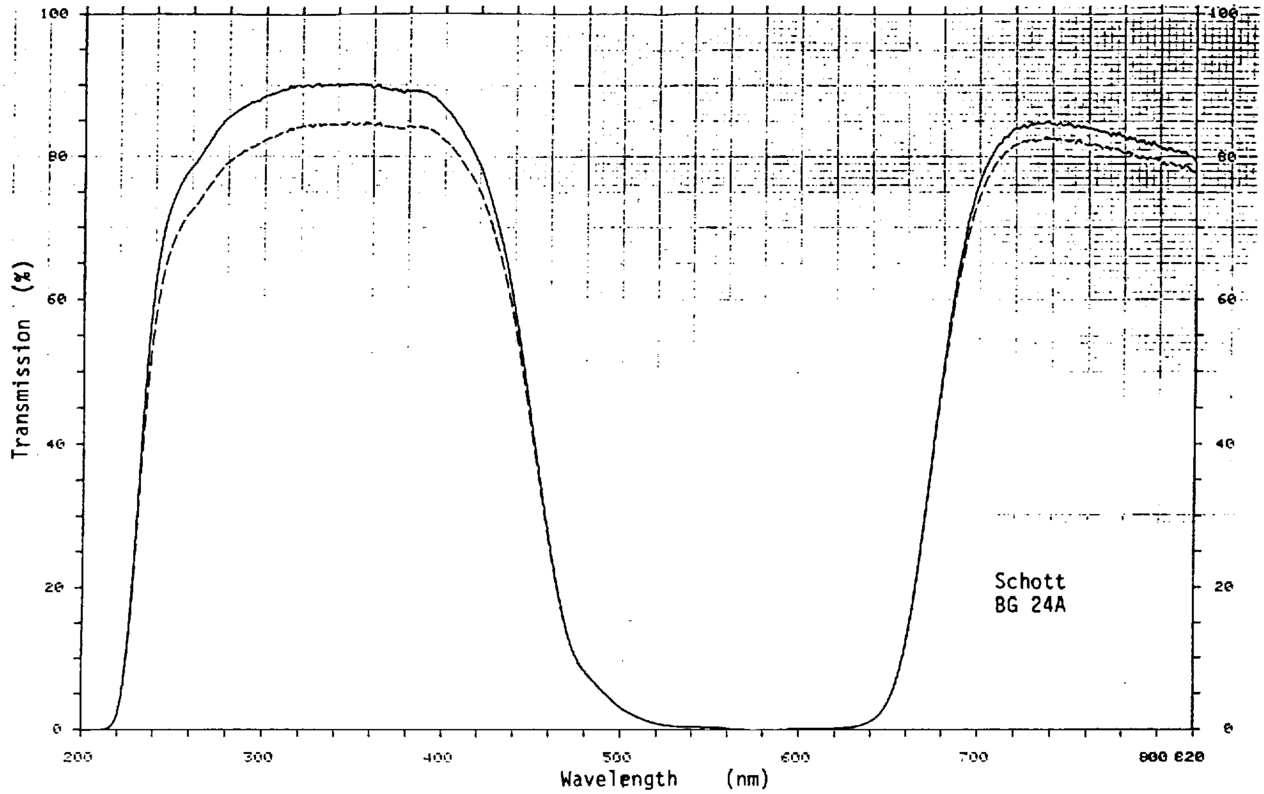
Transmission (%)
100
80
60
40
20
0
200
300
400
500
600
700
800 820
Wavelength (nm)
Schott
BG 24A

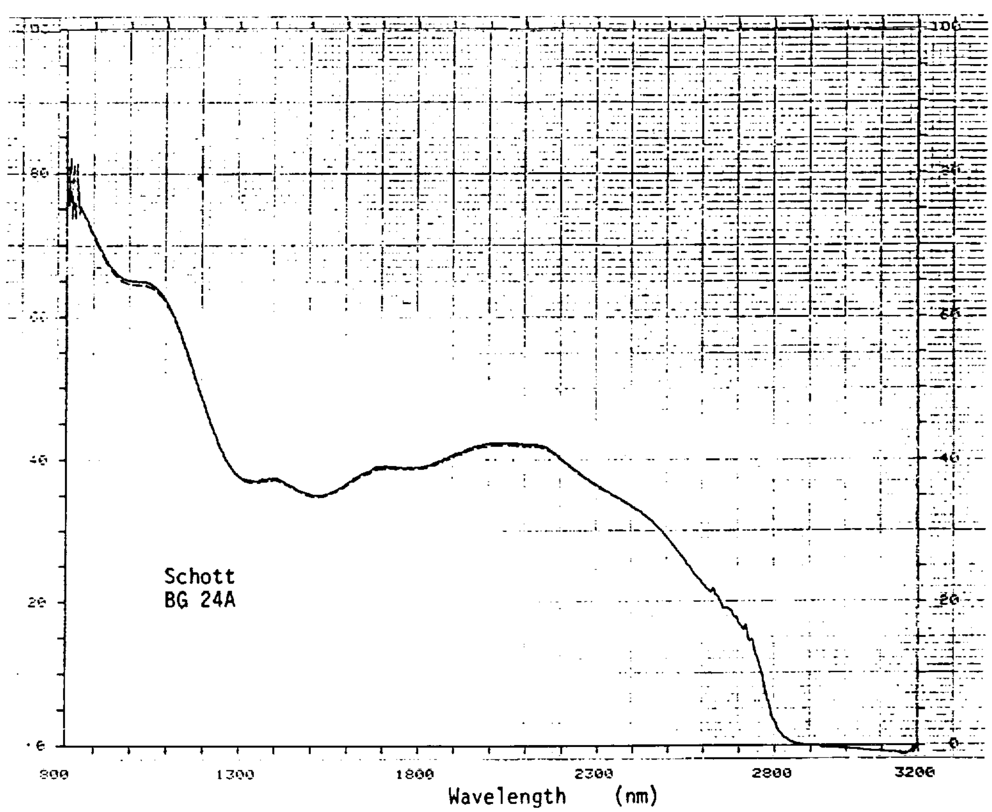
80
40
20
0
800
1300
1800
2300
2800
3200
Wavelength (nm)
Schott
BG 24A

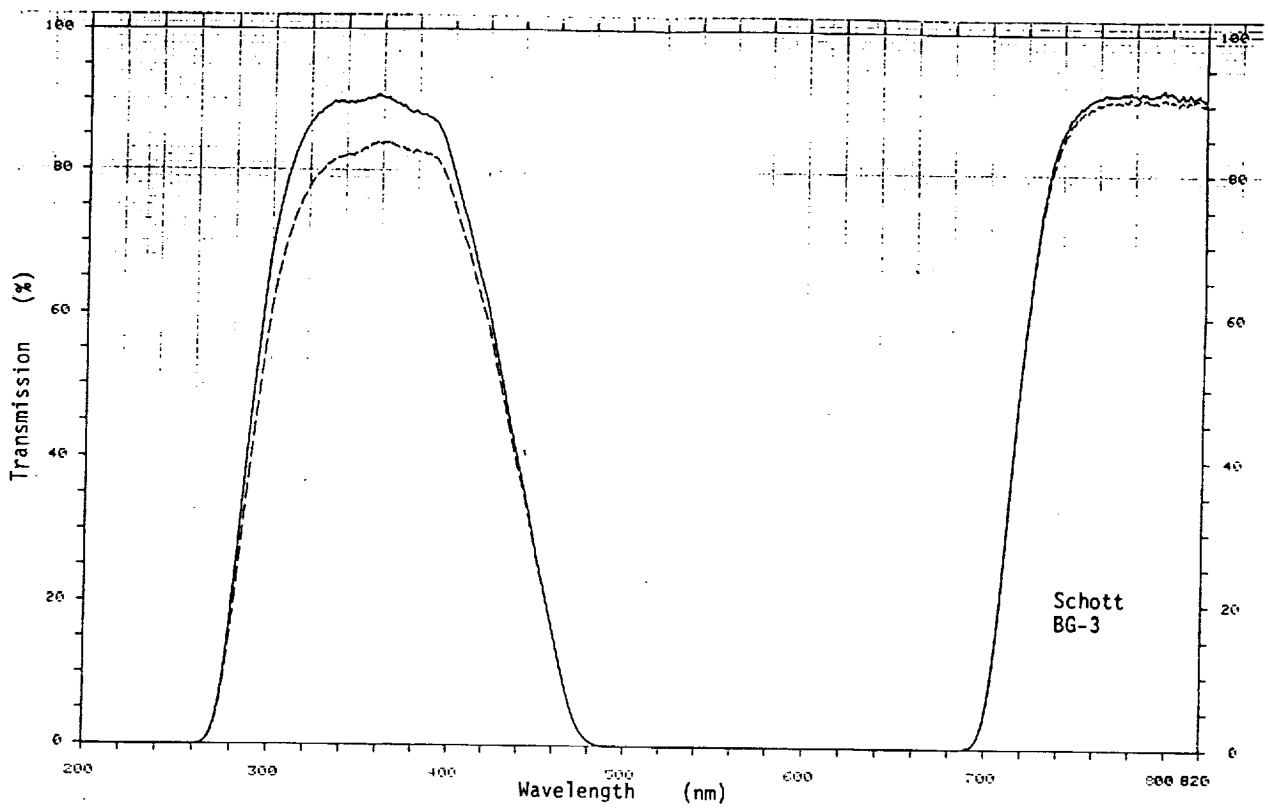
Transmission (%)
Wavelength (nm)
Schott
BG-3

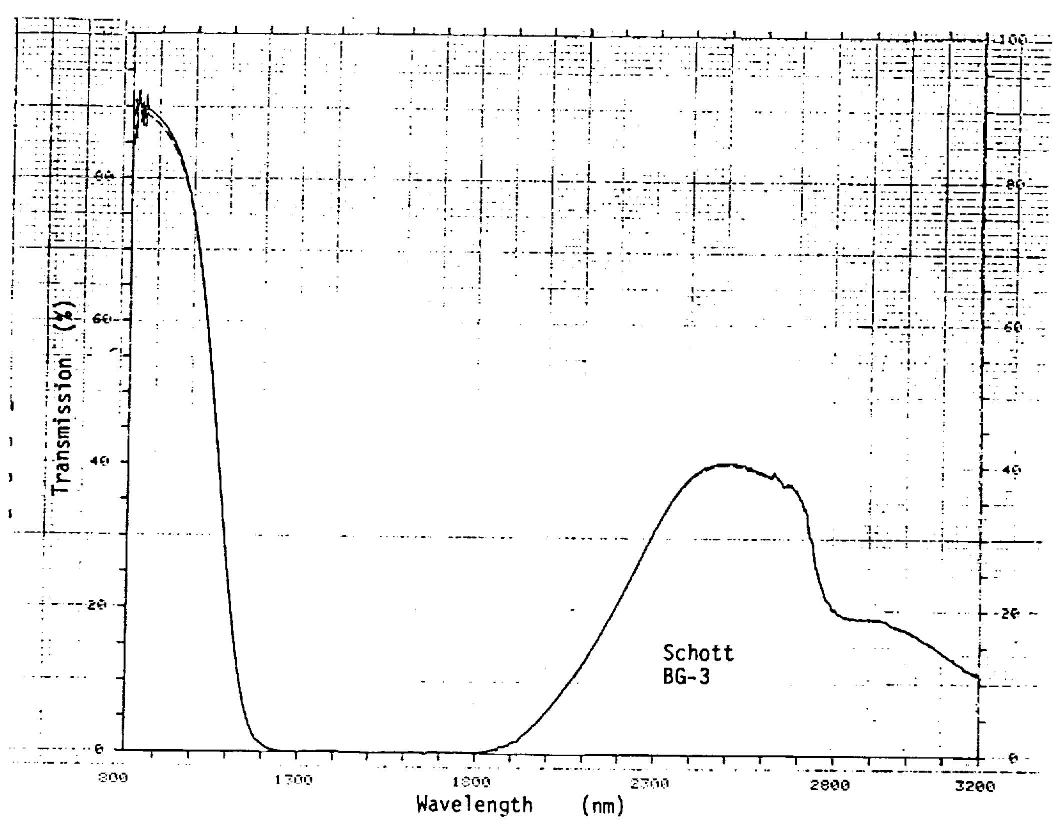
Transmission (%)
Wavelength (nm)
Schott
BG-3

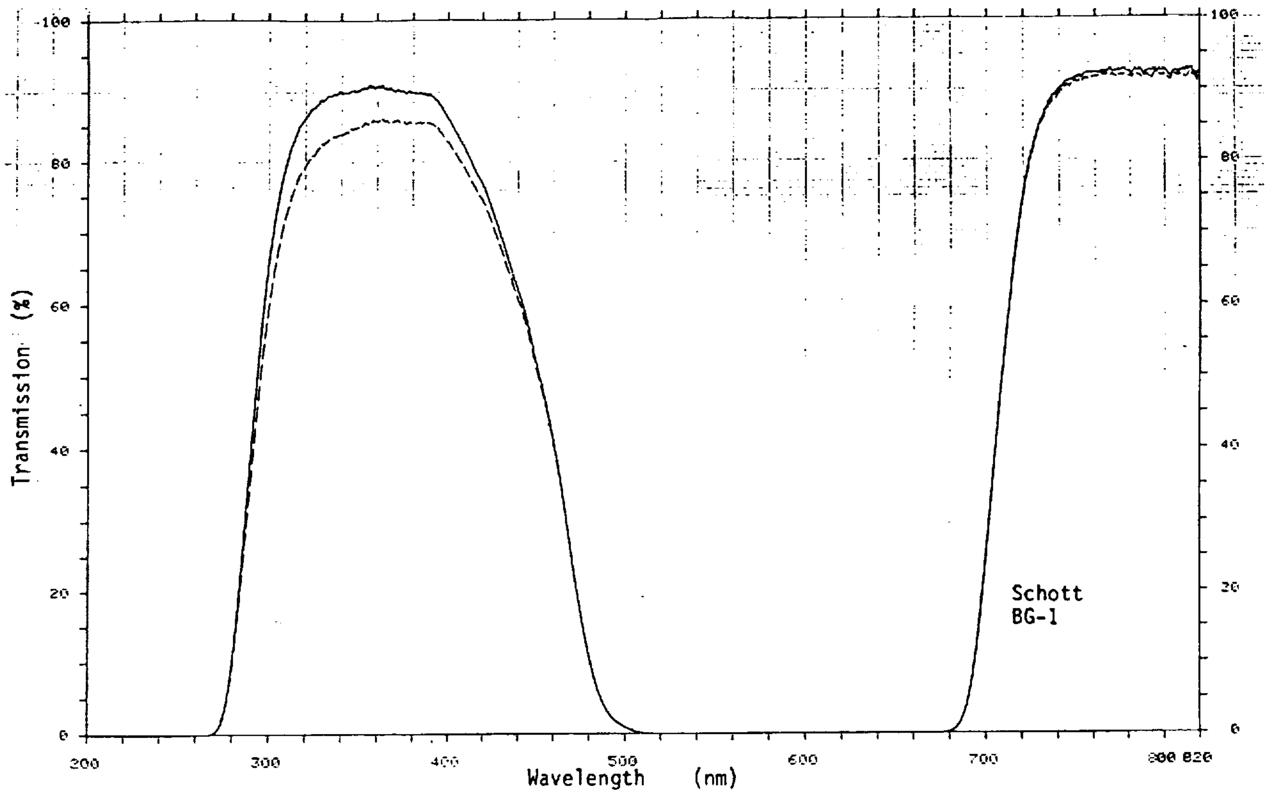
Transmission (%)
Wavelength (nm)
Schott
BG-1

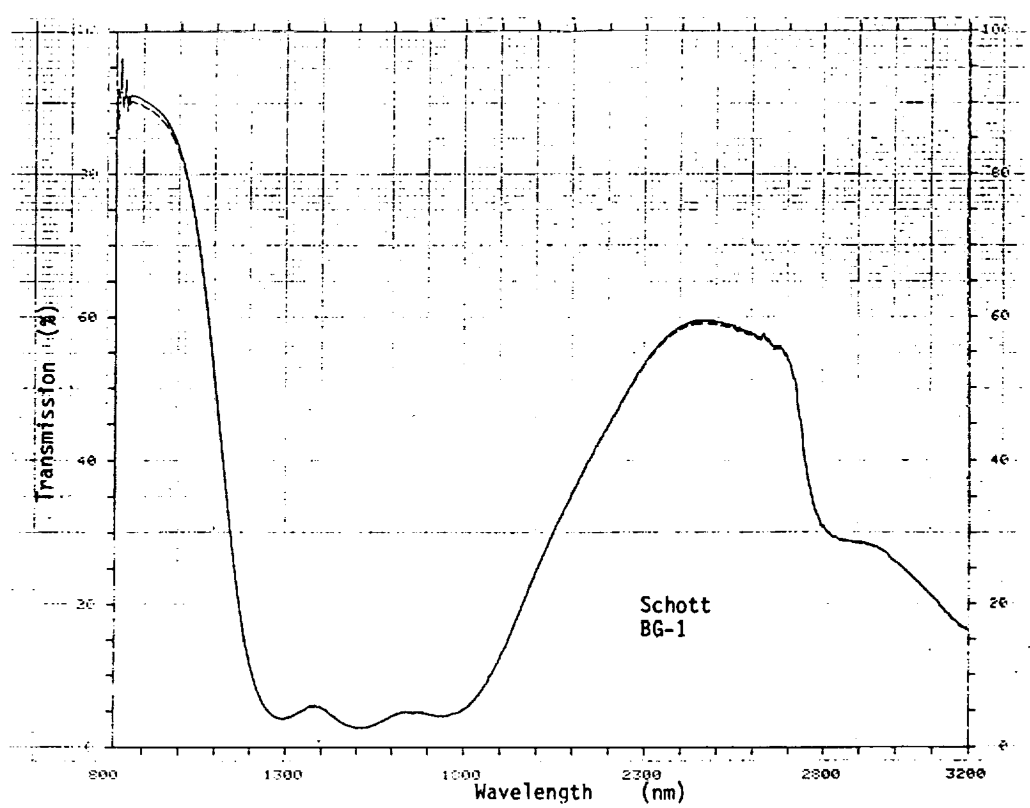
Transmission (%)
Wavelength (nm)
Schott
BG-1